UNIVERSIDADE FEDERAL DO CEARÁ
CENTRO DE CIÊNCIAS
DEPARTAMENTO DE BIOQUÍMICA E BIOLOGIA MOLECULAR
PROGRAMA DE PÓS-GRADUAÇÃO EM BIOQUÍMICA

MICAELLE RIBEIRO DOS SANTOS GOMES

ANÁLISE DE REDES E MODULAÇÃO METABÓLICA ASSOCIADAS A PARÂMETROS BIOQUÍMICOS E FISIOLÓGICOS EM CULTIVARES CONTRASTANTES DE ARROZ SOB SALINIDADE

FORTALEZA
2022

MICAELLE RIBEIRO DOS SANTOS GOMES

ANÁLISE DE REDES E MODULAÇÃO METABÓLICA ASSOCIADAS A PARÂMETROS BIOQUÍMICOS E FISIOLÓGICOS EM CULTIVARES CONTRASTANTES DE ARROZ SOB SALINIDADE

Dissertação apresentada ao Programa de Pós-graduação em Bioquímica da Universidade Federal do Ceará, como requisito parcial à obtenção do título de Mestre em Bioquímica.
Área de concentração: Bioquímica Vegetal

Orientador: Prof. Dr. Humberto Henrique de Carvalho.

FORTALEZA
2022

Dados Internacionais de Catalogação na Publicação
Universidade Federal do Ceará
Sistema de Bibliotecas
Gerada automaticamente pelo módulo Catalog, mediante os dados fornecidos pelo(a) autor(a)

G615a Gomes, Micaelle Ribeiro Dos Santos.
Análise de redes e modulação metabólica associadas a parâmetros bioquímicos e fisiológicos em cultivares contrastantes de arroz sob salinidade / Micaelle Ribeiro Dos Santos Gomes. – 2023.
82 f. : il. color.

Dissertação (mestrado) – Universidade Federal do Ceará, Centro de Ciências, Programa de Pós-Graduação em Bioquímica, Fortaleza, 2023.
Orientação: Prof. Dr. Humberto Henrique de Carvalho.

1. Salinidade. 2. Aclimatação. 3. Oryza sativa. 4. Metabolômica. I. Título.

CDD 572

MICAELLE RIBEIRO DOS SANTOS GOMES

ANÁLISE DE REDES E MODULAÇÃO METABÓLICA ASSOCIADAS A PARÂMETROS BIOQUÍMICOS E FISIOLÓGICOS EM CULTIVARES CONTRASTANTES DE ARROZ SOB SALINIDADE

Dissertação apresentada ao Programa de Pós-graduação em Bioquímica da Universidade Federal do Ceará, como requisito parcial à obtenção do título de Mestre em Bioquímica.
Área de concentração: Bioquímica Vegetal

Aprovada em: 08 /11 /2022.

BANCA EXAMINADORA

_____
Prof. Dr. Humberto Henrique de Carvalho (Orientador)
Universidade Federal do Ceará (UFC)

_____
Prof. Dr. Enéas Gomes Filho
Universidade Federal do Ceará (UFC)

_____
Profa. Dra. Giselle Camargo Mendes
Instituto Federal de Santa Catarina (IFSC)

À minha família, que sempre me influenciou
para ciência, por todo seu amor e paciência.
Amo vocês!

DEDICO

AGRADECIMENTOS

À Deus por presentear minha vida, estar em meu coração me guiando a ser uma pessoa melhor que fui ontem, fazendo meus erros, oportunidades para eu crescer.

À Minha mãe Aldenia por ter investido anos de cuidados e preocupações para me criar bem e contribuir em massa para eu ser quem sou hoje, por estar comigo nos momentos difíceis, por me inspirar com sua luta e nunca desistir mesmo nas adversidades, por conhecer meus sonhos e me ajudar a concretizá-los, por ouvir minhas esperanças, sentir meus problemas como seus e ser um grande exemplo para mim.

Ao meu pai Claudione por estar ao lado de minha mãe e juntos terem me criado, por entregar sua paciência e até bem-estar para assegurar o meu e de minhas irmãs, por ter me ensinado a ler e contar, por dividir seu conhecimento e sempre me incentivar a buscar mais.

À minha irmã Camila por ser minha primeira e de longe a melhor amiga que já tive, e por me aconselhar e proteger desde sempre.

À minha irmã Mirella por me alegrar com sua risada contagiante, fazer companhia quando mais preciso e dividir comigo seus momentos do dia a dia.

Ao Prof. Dr. Humberto Henrique de Carvalho por ser este grande exemplo de professor a ser seguido, um professor paciente e maravilhoso comigo, por dividir seu tempo em me orientar e tantos mais outros alunos que já orientou, e por toda sua experiência e conhecimentos que dividiu atenciosamente comigo.

Aos meus amigos e equipe do laboratório de fisiologia vegetal (LabFive), Dalton Oliveira, Marta Noronha, Italo Gomes, Rafael Costa, Lucas Pacheco, Savio Justino e Isabelle Pereira, pela boa convivência, apoio, ajuda e conhecimentos que dividiram comigo em toda a trajetória do mestrado.

À professora doutora Rosilene Mesquita por ter disponibilizado o IRGA e seus conhecimentos a respeito do funcionamento do equipamento tão importante para o presente trabalho.

Ao programa Conselho Nacional de Desenvolvimento Científico e Tecnológico – CNPq, por financiar meus estudos, o que ajudou bastante a fazer o presente trabalho.

RESUMO

A salinidade afeta o crescimento e desenvolvimento das plantas. No entanto há cultivares que apresentam tolerância maior do que outras, e hipotetiza-se que dispõem de metabólitos diferenciais que as permitem se aclimatar ao estresse salino evitando prejuízos ao rendimento. Deste modo, o objetivo do trabalho foi relacionar alterações morfológicas e bioquímicas com a modulação de metabólitos primários e o impacto na topologia das redes de duas cultivares de arroz, Esmeralda (ES) e São Francisco (SF) em hidroponia na ausência e presença de 80 mM de NaCl. Para isso, foi mensurado o comprimento da planta; massa seca; teor de clorofilas e carotenoides; trocas gasosas, fluorescência da clorofila *a*; íons inorgânicos; malondialdeído (MDA) e peróxido de hidrogênio; atividade de enzimas antioxidantes; e por fim, os perfis metabólicos. Os dados de metabólitos foram obtidos e analisados usando o software MetaboAnalyst para as análises multivariadas e Cytoscape para a criação de redes de correlação. Os resultados mostraram que as cultivares ES e SF submetidas à salinidade tiveram massa seca e comprimento reduzidos, bem como as trocas gasosas, clorofilas totais e carotenoides. No entanto, em todos os parâmetros supracitados, a cultivar SF apresentou reduções menores quando comparada com a ES. Em relação aos teores de MDA, a salinidade aumentou a peroxidação lipídica e a concentração de Na^+ foi maior na ES. Além disso, a SF apresentou maiores razões da relação K^+/Na^+ tanto nas folhas quanto nas raízes. Já as respostas metabólicas das duas cultivares sob estresse salino foram bastante distintas. Um total de 48 metabólitos foram identificados tanto na folha quanto na raiz. A análise de componentes principais mostrou uma clara separação entre os perfis dos tratamentos. Em geral, a quantidade de metabólitos alterados positivamente sob salinidade em folhas e raízes da SF foi maior comparativamente à ES de acordo com o test-t. A análise discriminante por mínimos quadrados parciais (OPLS-DA) revelou que na cultivar ES os metabólitos mais discriminantes foram ácido glicérico, palatinose e ácido treônico nas folhas enquanto leucina, fenilalanina e valina foram nas raízes. Para SF, arabinose, lisina e manose foram os discriminantes para folhas, e metionina, ornitina e xylitol foram os discriminantes para raízes. O efeito do sal impactou severamente as redes metabólicas nas folhas da ES, enquanto SF apresentou maior densidade e heterogeneidade. Por outro lado, as redes de metabólitos de raízes tiveram maior densidade para ambas as cultivares. A análise da rede incluindo o íon sódio revelou vários metabólitos correlacionados, sendo alguns deles confirmados pelo teste-t e OPS-DA. No geral, os dados mostraram que a ES apresentou um perfil metabólico

impactado negativamente pelo estresse salino, enquanto na SF esse impacto teve um efeito positivo nos quais vários metabólitos como carboidratos, aminoácidos e ácidos orgânicos foram induzidos sob salinidade, provocando melhor desempenho em comparação com ES e corroborando resultados fisiológicos e fenotípicos. Assim, esse estudo fornece novas informações sobre o mecanismo de aclimatação ao estresse salino e revela bases de modulação no metabolismo primário em cultivares de arroz que poderão ser usados para seleção de genótipos e no melhoramento genético para obtenção de plantas mais tolerantes a estresses ambientais.

Palavras-chave: salinidade; aclimatação; *Oryza sativa; m*etabolômica.

ABSTRACT

Salinity affects the growth and development of rice plants. However, some cultivars display better maintenance of features compared to others. We hypothesized that differential metabolites allow rice plants to acclimate to saline stress avoiding production losses. Thus, the main goal of this work was to relate morphological and biochemical alterations with the modulation of primary metabolites and the network topologies impact of two rice cultivars, Esmeralda (ES) and São Francisco (SF), under saline stress. Hydroponic plants were grown in the absence and presence of 80 mM NaCl. Then, length, dry masses, chlorophylls, carotenoid contents, gas exchange, inorganic ions, lipid peroxidation, hydrogen peroxide, antioxidant enzymes, and metabolite profiles were measured. Data were analyzed using MetaboAnalyst and Cytoscape to multivariates and network correlations. Salt stress promoted reductions of growth, total chlorophyll, carotenoid, CO_2 assimilation, and other photosynthetic traits in both cultivars but losses in the SF were lower than in ES. Otherwise, the lipide peroxidation, APX activity, and concentration of Na^+ were higher in ES leaves, while SF exhibited higher K^+/Na^+ in both leaves and roots. Metabolomic identified 48 metabolites as sugars, amino acids, organic acids, and others. Principal component analysis (PCA) showed a clear separation among treatment profiles in both leaves and roots. There was a positive metabolite modulation, especially for SF leaves and roots after salt treatment, corroborated by the t-test. Orthogonal Partial Least Squares Discriminant (OPLS-DA) analysis revealed that in the ES most discriminating were glyceric acid, palatinose, and threonic acid that were positive in leaves while leucine, phenylalanine, and valine were positive in roots. For SF, arabinose, lysine, and mannose were the discriminants for leaves, and methionine, ornithine, and xylitol were the discriminants for roots. The effect of salt severely impacted the network of ES leaves, while SF exhibited higher density and heterogeneity. The networks from root metabolites had more density for both cultivars. The network that included sodium ion revealed several metabolites correlated, in which some of them were confirmed by t-test and OPS-DA. Overall, our data showed that ES presented a metabolic profile negatively impacted by salt stress whilst SF this impact had a positive effect in which several metabolites such as carbohydrates, amino acids, and organic acids were induced under salt treatment leading to a better performance in comparison to ES and corroborated physiological results. Thus, this study provides new insights into the mechanism of acclimatization to salt stress and indicates bases of modulation in primary metabolism in rice cultivars that can be used for genotype

selection and genetic breeding programs to develop plants more tolerant to environmental stresses.

Keywords: salinity; acclimatization; *Oryza sativa*; metabolomics.

LISTA DE ILUSTRAÇÕES

LISTA DE TABELAS

LISTA DE ABREVIATURAS E SIGLAS

A-	CO_2 Assimilation
A/Ci-	Efficiency of ribulose-1,5-bisphosphate carboxylase/oxygenase (Rubisco)
ANOVA-	Variance analysis
Chl a-	Chlorophyll *a*
Chl b-	Chlorophyll *b*
Chl t-	Total chlorophylls
DM-	Dry mass
DSPC-	Debiased sparse partial correlation
EI-	Electron Ionization
ES-	Rice BRS Esmeralda
ES-CNT-	Rice BRS Esmeralda in control
ES-SALT-	Rice BRS Esmeralda in salt
ETR-	Electron Transfer Rate
gs-	Stomatal Conductance
IRGA-	Infrared Gas Analyser
KEGG-	Kyoto Encyclopedia of Genes and Genomes pathway
MDA-	Malondialdehyde
NIST-	National Institute of Standards & Technology
OPLS-DA-	Orthogonal Partial Least Squares-Discriminant Analysis
PCA-	Principal Component Analysis
RDM-	Root Dry Mass
PQ-	Photochemical quenching
RL-	Root length
SF-	Rice BRS São Francisco
SF-CNT-	Rice BRS São Francisco in control
SF-SALT-	Rice BRS São Francisco in salt
SL-	Shoot Length
SISVAR-	Statistical analysis and design of experiments program.
SOS-	Salt Overly Sensitive
Trmmol-	Transpiration
VIP scores-	Variable Importance in Projection

SUMÁRIO

1 INTRODUÇÃO

1.1 Cultura de arroz e importância econômica

O arroz (*Oryza sativa* L.) compõe a dieta de mais da metade da população mundial, e sua produção alcança cerca de 519,5 milhões de toneladas (FAO, 2022). Fora do continente asiático, o Brasil é o país que mais produz arroz, ocupando cerca de 1.619,8 mil de hectares de área cultivada, sendo 1.302 mil hectares de área de arroz irrigado e 317,8 mil hectares de sequeiro, e gerando anualmente quase 11 milhões de toneladas de grãos (CONAB, 2022). Sua produção pode ser feita sob dois sistemas: Sequeiro ou "cultivo em terras altas", que são solos com boa drenagem e dependentes da precipitação pluviométrica; E o irrigado, onde a produção do arroz se dá por inundação (FAGERIA, 2001; EMBRAPA, 2020), que pode ser controlada, através da manutenção constante da lâmina de água, ou sem irrigação controlada, na qual a produção de arroz é feita em terras baixadas, onde há acumulo de agua por chuvas, rios ou lençol freático para o desenvolvimento da orizicultura (CONAB, 2015).

A produção de arroz irrigado pode ser problemática, pois pode contribuir para a emissão de metano (EMBRAPA, 2020), neste sentido a Embrapa produziu uma cultivar de arroz destinado a terras altas, a BRS Esmeralda (ES). Esta cultivar é oriunda do cruzamento entre a linhagem CNAx4909-68-MM2-PY2 e a cultivar BRS Primavera, e apresenta grãos longos e finos, baixo teor de amilose, maciez, boa soltabilidade e facilidade de cozimento, e suas plantas podem chegar a uma altura de 95 a 108 cm com perfilhamento moderado e área foliar mediana. Sua fisiologia propicia maior rendimento comparada às cultivares tradicionais por possuir forte auto sombreamento, presença de senescência tardia, que reduz o risco de acamamento, alto vigor, alta competição com plantas daninhas, elevada tolerância a estresses abióticos, tais como condições ruins de solo e clima, além de apresentar resistência a doenças como brusone na panicula. A ES foi destinada ao plantio nas regiões Norte (Pará, Roraima, Rondônia e Tocantins), Nordeste (Maranhão e Piauí), Sudeste (Minas Gerais) e Centro-Oeste (Mato Grosso e Goiás) (EMBRAPA, 2014). Diferente da ES, a cultivar BRS São Francisco (SF) foi criada com destino ao sistema irrigado, com controle da lâmina de água, e produzido massivamente na região Nordeste (Alagoas, Sergipe e Pernambuco). Esta cultivar é oriunda do cruzamento entre as linhagens 5732 e 3234 COSTA RICA, e também apresenta grãos longos e finos, alto teor de amilose, maciez, boa soltabilidade sem necessidade de muita agua no cozimento, e suas plantas apresentam altura média de

80 cm com perfilhos semi compactos, e plantas com folhas curtas e eretas com resistente ao acamamento e ao brusone na folha e na panícula, mas podendo apresentar mancha parda (*Helminthosporium oryzael*) em condições de deficiência hídrica (EMBRAPA, 2000).

1.2 Salinidade e estresse salino nas plantas

Além de contribuir para a diversidade ecológica e sustentabilidade da vida na Terra, as plantas influenciam diretamente na economia mundial, sendo que a demanda por alimento, fibras, combustíveis e outros derivados aumenta a cada ano (WAADT *et al.*, 2022). No entanto o crescimento e produtividade são constantemente prejudicados pela intensidade e duração tanto de estresses bióticos decorrentes de vírus, fungos, bactérias, predadores e parasitas (MELO *et al.*, 2022) quanto abióticos, tais como seca, salinidade, calor e frio, os quais podem ser intensificados diante do cenário de mudanças climáticas (WAADT *et al.*, 2022). Alguns desses estresses raramente estão presentes na vida das plantas, enquanto outros, tais como seca e salinidade, são recorrentes, e estão entre as principais variáveis ambientais que provocam perdas consideráveis na produção agrícola (SHARMA *et al.*, 2022). A salinidade ocorre principalmente em climas áridos e semiáridos, agravados pela baixa pluviosidade e uma irrigação falha em drenagem e evaporação intensa da água, levando ao acúmulo de íons na superfície (SHAHID; ZAMAN; HENG, 2018; ZAMLJEN *et al*., 2022). O problema da salinização dos solos é verificado principalmente na região Nordeste, onde aproximadamente 25% das áreas irrigadas estão salinizadas tanto por técnicas inadequadas quanto pela baixa precipitação (PEDROTTI *et al*., 2015).

No Brasil, o Rio Grande do Sul (RS), responsável por até 70,7% da produção nacional de arroz (IBGE 2022), no qual a maioria do cultivo de arroz se dá pela forma irrigada, apresenta variações de Condutividade Elétrica (CE), referente à concentração total de íons sódio existentes na água, que varia de 0,93 a 10,5 $dS.m^{-1}$ (micro Siemens por metro) em seus principais rios destinados a orizicultura (Figura 1) (DENARDIN *et al.*, 2020), e o solo é capaz de absorver a salinidade desta água.

Os rios do RS podem apresentar aproximadamente 80 mmol kg^{-1} (ou 80 mM) de NaCl (Figura 1), e de acordo com a literatura, o solo pode ser considerado salino quando a condutividade elétrica alcança 40 mM de NaCl (equivalente a 4 $dS.m^{-1}$) (SHAHID; ZAMAN; HENG, 2018; ZAMLJEN *et al.*, 2022), e altos teores de

sal podem provocar severos danos ao crescimento e diminuir o desenvolvimento dessas plantas (HUSSAIN *et al.*, 2021).

Figura 1: Correlação entre CE e molalidade do íon sódio nos principais rios do RS.

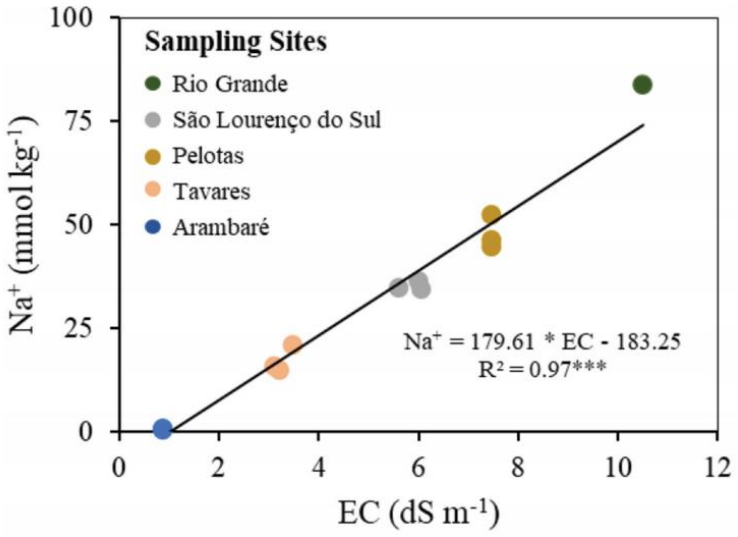

Fonte: Denardin *et al*. (2020)

A salinidade presente nos meios de cultivo pode desencadear uma série de estresses fisiologicamente relacionados, como o estresse osmótico, sendo causado por altas concentrações de Na^+ e Cl^- no solo, que reduzem o potencial osmótico da solução do solo, dificultando a absorção de água pelas raízes das plantas, no qual influencia negativamente no fluxo de água e sais no xilema, culminando em alterações morfofisiológicas, tais como a diminuição da área foliar, comprimento e massa fresca e seca das plantas (NASEER *et al*., 2022). Por exemplo, a aplicação de estresse salino (150 mM de NaCl) em feijão (informe o genótipo ou cultivar) foi capaz de diminuir significativamente o comprimento da parte aérea (CPA) e da raiz (CR) em 14,8% e 26,6%, respectivamente. Também, da mesma forma, diminuiu a massa fresca da parte aérea (MFPA), a massa seca da parte aérea (MSPA) e as massas fresca e seca da raiz (MFR e MSR) do feijão (TANIA *et al.*, 2022).

O estresse salino também é capaz de causar alterações bioquímicas, como a inibição fotossintética (HASANUZZAMAN; FUJITA, 2022), visto que o estresse osmótico resulta no fechamento estomático rápido, a fim de minimizar a perda de água pela transpiração (CHEN *et al*., 2021), o que reduz a capacidade da planta de assimilar gás carbônico (CO_2) (LIU, C. *et al*., 2022), causando o estresse oxidativo (FAL *et al*., 2022) pela produção de elétrons de alta energia, que são sucessivamente transferidos

para moléculas de O_2 levando à produção de espécies reativas de oxigênio (EROs) (ALAM *et al*., 2022).

As EROs normalmente atuam como moléculas sinalizadoras, mas em excesso podem provocar danos oxidativos, tais como peroxidação lipídica e perda de pigmentos fotossintéticos (SILVA *et al.,* 2022), que influenciam diretamente na capacidade fotossintética das plantas (SHERIN; ASWATHI; PUTHUR, 2022).

Além de causar perda de clorofila e carotenoides, as EROs também atuam nos ácidos graxos que fazem parte dos lipídios das membranas celulares, gradualmente os decompondo em uma série de compostos, incluindo o malondialdeído (MDA), e sua detecção pode refletir no nível de oxidação lipídica (YANG *et al.,* 2022).

Assim, é importante entender os mecanismos de aclimatação e tolerância pelos quais as plantas respondem e prosperam sob condições de estresse salino para desenvolver abordagens alternativas que garantem a produtividade e o suprimento alimentar (MITTLER *et al.,* 2022), tais como a hibridização interespecífica de plantas bastante tolerantes à salinidade (halófitas) por meio de abordagens genéticas ou melhorando vegetal para desenvolver de culturas mais tolerantes (HASANUZZAMAN; FUJITA, 2022).

1.3 Mecanismos de tolerância em plantas

As plantas, por serem organismos sesseis, tiveram que desenvolver mecanismos sofisticados para perceber, reagir aos estresses e se adaptar de forma eficiente (WAADT *et al.,* 2022). Os principais mecanismos de tolerância ao sal incluem, por exemplo, a eliminação de EROs e a homeostase iônica (HUSSAIN *et al.*, 2021). A fim de evitar os danos das EROs, as células vegetais controlam a homeostase desses radicais através do sistema antioxidante, composto sobretudo por enzimas, tais como a superóxido dismutase (SOD), a catalase (CAT), a peroxidase do ascorbato (APX), dentre outras (MANSOOR *et al.,* 2022). A SOD é a primeira linha de defesa contra os danos mediados por ROS, catalisando a desproporção de radicais livres superóxido ($\bullet O_2^-$) para gerar peróxido de hidrogênio (H_2O_2) e O_2. O peróxido de hidrogênio, por sua vez, é eliminado pelas enzimas CAT e APX (MANSOOR *et al.*, 2022; YANG *et al.,* 2022). O sistema antioxidante não-enzimático complementa e auxilia no processo de eliminação das EROs, e é composto por vitaminas, tais como a vitamina E e o ascorbato, carotenóides, e a glutationa oxidada (GSH) e reduzida (GSSG) (HASANUZZAMAN *et al*., 2019).

Além de ativar o mecanismo antioxidante, e minorar o estresse oxidativo secundário, outra forma de mitigar os efeitos do estresse salino é através da homeostase iônica, uma vez que o excesso desses íons causa toxicidade celular, e interfere na absorção e metabolismo de íons fundamentais para a tolerância ao sal, tal como o K^+, essencial para o crescimento dos organismos vegetais (CHEN *et al.*, 2021). Em arroz, a via de sinalização *Salt Overly Sensitive* (SOS) é ativada sob estresse salino, com a ativação dos genes *OsSOS1*, que indiretamente medeiam a absorção de Na^+ radicular, sua redistribuição nos brotos, e seu efluxo do citoplasma para o apoplasto (CHEN *et al.*, 2021). Entretanto este processo, que é mediado por SOS1, consome energia e é acompanhado pela atividade da H^+-ATPase, que é uma bomba de prótons integrada a membrana plasmática, capaz de gerar um gradiente eletroquímico de H^+ para impulsionar a exlusão de Na^+ através do consumo de ATP (FAN *et al.*, 2019; XIE; ZHOU; JIANG, 2022). Outro mecanismo encontrado nas plantas é o sequestro dos íons Na^+ no vacúolo por meio de transportadores antiporte Na^+/H^+ (NHXs) localizado no tonoplasto (APSE; BLUMWALD, 2007; SOLIS *et al*., 2022), que retiram Na^+ bombeando H^+ para o vacúolo, através de duas bombas de prótons vacuolares: H^+-pirofosfatase (V-PPase, E.C. 3.6.1.1) e H^+-ATPase (V-ATPase, E.C. 3.6.1.3). E quando o arroz superexpressa as NHXs, aumenta a capacidade de reter íons K^+, garantindo tolerância à salinidade (FLOWERS; COLMER, 2008; SOLIS *et al*., 2022). Essas H^+-ATPases podem ser de membrana plasmática (tipo P) e vacuolar (tipo V), que exercem a mesma função de bombear prótons, mas em localidades diferentes da célula, participando do crescimento em respostas às mudanças no ambiente, tais como o estresse (LI Y *et al*., 2022). Além dos transportadores do tipo antiporter, os vegetais podem mediar o influxo de sódio através das membranas plasmáticas, que possuem receptores (receptores de glutamato (GLRs)), transportadores (transportadores de K^+ de alta afinidade (HKTs), transportador de Arabidopsis K^+ (AKT1), e canais iônicos (canais de cátions não seletivos (NSCCs)) em sua composição, (SHAH *et al*., 2021; BACHANI *et al*., 2022). Deste modo, é possível evitar o acúmulo de Na^+ tecidual, manter o teor de clorofila, atividade fotossintética, potenciais hídricos das folhas dentre outros processos vitais para a célula (MUNNS *et al*., 2016; SOLIS *et al*., 2022).

Regular a absorção dos íons salinos (homeostase iônica) evita a toxicidade iônica, e garante solutos suficientes para o ajuste osmótico (MUNNS; GILLIHAM, 2015; MUNNS *et al*., 2020). Ajustes osmóticos também fazem parte dos

mecanismos de tolerância ao sal, acumulando solutos compatíveis, tais como prolina e trealose, ou superexpressando genes envolvidos na produção desses osmólitos, tais como a trealose-6-fosfato sintase (TPS) e trealose-6-fosfato fosfatase (TPP), relacionados à produção de trealose, a fim de aliviar a pressão osmótica induzida pela elevada concentração de sais (CHEN *et al.,* 2021), e proteger as membranas plasmáticas e proteínas sob estresse (POONAM *et al*., 2016; SINGH *et al*., 2022), sendo que a transferência do gene TPP do arroz em plantas de milho foi capaz de aumentar a produção de 20% a 31% (NUCCIO *et al*., 2015; SINGH *et al*., 2022). Outros osmólitos como álcoois de açúcares (pinitol, manitol, mio-inositol e sorbitol), além de participar de ajustes osmóticos, também estão envolvidos na regulação do dano oxidativo (BHATTACHARYA; KUNDU, 2020; SINGH *et al*., 2022). O osmoprotetor manitol também pode atuar metabolizando radicais hidroxila (GILL; TUTEJA, 2010; SINGH *et al*., 2022), e foi relatado que plantas transgênica de *Populus tomentosa* superexpressam o gene mtlD, que codifica a enzima manitol-1-fosfato desidrogenase que converte manitol-1-fosfato em manitol foi responsável pelo aumento da tolerância ao estresse salino, por aumentar a proteção ao EROs (HU *et al*., 2005; SINGH *et al*., 2022). O 21xigenas e mio-inositol, apresentam osmoproteção (HANDA *et al.*, 2018; SINGH *et al*., 2022). Adicionalmente, os osmólitos participam na produção de fitohormônios (ex.: auxina) e ácido fítico, atuando ainda na proteção da planta (HAZRA *et al*., 2019; SINGH *et al*., 2022), protegendo suas organelas contra as EROs e aliviando a pressão de turgor celular dentro da célula (MAJUMDER *et al*., 1997; SINGH *et al*., 2022). E as poliaminas (PAs) (espermidina (Spd), putrescina (Put) e espermina (Spm)) também podem atuar na manutenção do ajuste osmotico, além de mitigar o efeito das EROs, aumentam a fluidez da membrana e disponibilizam nitrogênio para as plantas, dentre outras funções (CHEN *et al*., 2019; SINGH *et al*., 2022).

Além dos parâmetros bioquímicos supracitados e observados na adaptação das plantas ao estresse salino, os mecanismos de tolerância geralmente envolvem uma cascata de moléculas de sinalização, capazes de modular a expressão de genes específicos, que podem codificar proteínas envolvidas em funções metabólicas ou regulatórias diferencialmente expressas em resposta aos estresses (BASHIR *et al*., 2021). Em uma pesquisa envolvendo variedades de batata-doce com tolerância diferencial ao déficit hídrico, foi possível observar um total de 97 proteínas expressas diferencialmente expressas na variedade tolerante à seca, tais como a enzima peroxidase de ascorbato, proteína de ligação de clorofila, a subunidade grande da ribulose-1,5-

bifosfato carboxilase/22xigenasse, protease do tipo cisteína e Mn-SOD, sendo estas proteínas envolvidas no metabolismo fotossintetico, produção de energia e regulação de EROs (ZHOU *et al*., 2022).

Além de genes e proteínas, as plantas também modulam uma ampla gama de metabólitos encarregados de vários aspectos do crescimento e desenvolvimento sob estresse e também no ajuste osmótico (ZANDALINAS *et al*., 2022). Há alterações metabólicas acompanhadas de mudanças fisiológicas que podem fornecer informações importantes sobre como as plantas toleram o estresse (SANTOS *et al.,* 2022). Por exemplo, em uma pesquisa envolvendo cultivares de pimenta sob salinidade (20 e 40 mM de NaCl) houve modulação de metabolitos responsivos ao estresse com diminuição de sacarose, glicose, frutose, ácidos orgânicos e aminoácidos (ZAMLJEN *et al.*, 2022).

Neste sentido, abordagens ômicas, tais como genômica, transcriptômica, proteômica e metabolômica, podem ajudar a entender os mecanismos de resposta desencadeados pelas plantas sob estresses (SHU *et al.*, 2022).

1.4 Tecnologias “ômicas” para o estudo de estresse em plantas

Tecnologias ômicas são bastante aplicadas no estudo de plantas (YAN *et al.*, 2022). A transcriptômica, que estuda o conjunto de moléculas de RNA (transcritos) diferencialmente expressa em uma determinada amostra (célula, tecido ou organismo), produz informações úteis quanto a regulação de mecanismos celulares por meio da expressão gênica específica (PAGE; LAWLEY, 2022). Essa técnica ômica é bastante aplicada em estudos que buscam investigar os transcritos diferencialmente expressos em uma planta tolerante e uma sensível (WANG W. *et al.*, 2022). A proteômica é outro exemplo de tecnologia ômica, na qual busca identificar o conjunto de proteínas de um organismo. Este estudo é bastante útil por ser possível descobrir biomarcadores para estímulos específicos, e/ou determinar vias biológicas, mecanismos moleculares e redes funcionais em seus respectivos níveis de organização biológica (célula, tecido, órgão, dentre outros) (YAN *et al.*, 2022). Assim como a transcriptômica, a proteômica também pode ser usada para investigar proteínas responsivas ao estresse (como proteínas da categoria de glicólise, desintoxicação de EROs, transporte, sinalização, metabolismo de aminoácidos, dentre outros (KHAN *et al.,* 2022)) a fim de compreender melhor os mecanismos moleculares regulados sob estresse por plantas com tolerância diferencial (LI, X. *et al.*, 2022).

A metabolômica busca identificar metabólitos, tais como aminoácidos, carboidratos, lipídios, peptídeos e ácidos orgânicos (MORZE *et al.*, 2022), alterados em resposta ao estresse abiótico e biótico (XIAO *et al.*, 2022).

Os metabólitos podem ser divididos em primários e secundários. O primeiro diz respeito aos componentes básicos necessárias para o crescimento e desenvolvimento dos vegetais, enquanto os metabólitos secundários estão presentes apenas em um determinado estágio ou período de crescimento das plantas. E a investigação desses metabólitos (primários e/ou secundários) pode ser feita pela técnica de metabolômica direcionada ou não direcionada. A técnica direcionada está relacionada à utilização do metabolito conhecido através de métodos de extração específicos e padrões de alta pureza a fim de quantificar o metabólito alvo. No entanto, a desvantagem deste método é que há quantificação de poucos metabólitos. Por outro lado, a técnica metabolômica não direcionada, envolve a quantificação do máximo de metabólitos que tem na amostra de forma desconhecida (LI, J. *et al.*, 2022).

A técnica metabolômica de plantas é bastante complexa e necessita de um projeto experimental que envolve a coleta, processamento e preparação das amostras para a sucessiva detecção e análise dos dados. A técnica de detecção dos dados comumente usada é a cromatografia gasosa (aplicada na separação de metabólitos) acoplada à espectrometria de massa para detecção metabólica (XIAO *et al.*, 2022). Nesta técnica as áreas dos picos resultantes são normalizadas por um padrão interno e o valor relativo do metabolito é determinado (APRIYANTO *et al.*, 2022). Posteriormente é realizado o tratamento desses dados por meio de softwares como, por exemplo, o Xcalibur (LEGRAND *et al.*, 2022) e a análise estatística é feita no MetaboAnalyst. Tal análise estatística pode ser univariada (duas variedades estatísticas) para dados de dois grupos (ex.: testes t) ou para dados de vários grupos (ex.: ANOVA); ou análise multivariada (análises simultâneas de mais de duas variáveis estatísticas), que também inclui ANOVA, análise de componentes principais (PCA), dentre outros (CHEN *et al.*, 2022). O PCA demonstra a reprodutibilidade em grupos de dados e suas diferenças. Outras análises semelhantes ao PCA são a análise discriminativa de mínimos quadrados parciais (PLS-DA) e projeções ortogonais para estruturas latentes (OPLS-DA), ambas minimizam a dimensionalidade dos dados e os analisam com um modelo de regressão entre expressão metabólica e relações de agrupamento, que enfatizam melhor as diferenças intergrupos, possibilitando a identificação de biomarcadores em determinado tratamento (XIAO *et al.*, 2022).

Sendo os dados metabólicos tão grandes e complexos, eles podem ser interpretados biologicamente, e além do MetaboAnalyst, outro programa amplamente utilizado para a análise desses dados é o Cytoscape (PILON *et al.,* 2021). Nesta abordagem, os metabólitos correspondem a nós, que aparecem conectados por meio de arestas formando redes moleculares. Nestas redes, os nós se relacionam através de vias metabólicas e reações enzimáticas passíveis de sugestões quanto a metabólitos co-regulados (AMARA *et al.,* 2022). A força das conexões dos nós pode ser mediada através de um limite específico do coeficiente DSPC (*r*) e os parâmetros analisados na rede podem ser a heterogeneidade da rede, a densidade da rede, os componentes conectados, dentre outros (FREIRE *et al*., 2021).

Assim, a utilização de tecnologias “ômicas” são de extrema importante para o entendimento dos mecanismos de tolerância e a sensibilidade à salinidade em folhas e raízes de plantas de arroz associadas às alterações morfofisiológicas e bioquímicas. Isso permitirá que novas ideias possam surgir para a seleção de cultivares com melhor desempenho, bem como contribuir positivamente para o desenvolvimento das plantas de arroz mais tolerantes por meio da engenharia genética.

2 HIPÓTESE

Diante do exposto levantou-se a hipótese que plantas de arroz da cultivar BRS São Francisco, considerada tolerante à salinidade em relação a cultivar BRS Esmeralda, apresentam perfil metabólico e redes moleculares diferenciais que permitem a aclimatação ao estresse salino, corroborando com os dados morfofisiológicos (comprimento e massa seca) e bioquímicos (eficiência fotossintética, teor de clorofilas, atividade enzimática, teor iônico e produção de EROs).

3 OBJETIVOS

3.1 Objetivo geral

- Relacionar alterações morfológicas e bioquímicas com redes moleculares e modulação de metabólitos primários de duas cultivares de arroz, BRS Esmeralda (ES) e BRS São Francisco (SF), com tolerância diferencial ao estresse salino.

3.2 Objetivos específicos

Utilizando-se plantas de arroz das cultivares ES e SF sob condições controle (NaCl 0 mM) e de salinidade (NaCl 80 mM), pretende-se:

- Determinar os comprimentos da parte aérea e das raízes;
- Determinar as massas secas das folhas, raízes, caules e da planta inteira;
- Quantificar os teores de clorofilas e carotenoides;
- Avaliar as trocas gasosas: Assimilação de CO_2 (*A*), condutância estomática (*gs*), eficiencia da ribulose-1,5-bisfosfato carboxilase/oxigenase (Rubisco) (*A*/Ci) e transpiração (Trmmol);
- Medidas de fluorescência da clorofila a: Taxa de transferência electrônica (ETR), extinção fotoquímica (PQ), extinção não fotoquímica (NPQ) e rendimento quântico do fotossistema II (PSII) (Fv/Fm);
- Mensurar os teores de íons Na^+ e K^+ nas folhas e raízes;
- Quantificar os teores de MDA e H_2O_2 nas folhas;
- Determinar a atividade enzimática da CAT e APX nas folhas;
- Determinar os perfis metabólicos foliares e radicular;
- Avaliar as redes metabólicas;
- Analisar os parâmetros de rede dos metabólitos responsivos ao estresse.

4 MANUSCRITO

4.1 Title: METABOLIC MODULATION AND NETWORKS CORROBORATE THE BETTER PERFORMANCE OF THE SÃO FRANCISCO RICE CULTIVAR UNDER SALINITY IN RELATION TO THE ESMERALDA CULTIVAR

4.2 Abstract

Under salinity, some rice cultivars show differential tolerance. We hypothesized that differential metabolites allow plants to acclimate to saline stress avoiding production losses. Thus, the main goal of this work was to evaluate changes in growth, biochemical, modulation of primary metabolites, and the network topologies of rice Esmeralda (ES) and São Francisco (SF) cultivars under the absence and presence of 80 mM NaCl. Salt stress promoted reductions of morpho-physiological and biochemical traits, but losses in the SF were lower than in ES. SF exhibited higher K^+/Na^+ in both leaves and roots. There were distinct profiles and a positive metabolite modulation, especially for SF leaves and roots after salt treatment. The top three discriminating metabolites were glyceric acid, palatinose, and threonic acid for ES leaves, while leucine, phenylalanine, and valine were for ES roots. For SF, arabinose, lysine, and mannose were the discriminants in leaves, and methionine, ornithine, and xylitol were the discriminants in roots. Salinity severely impacted the network of ES leaves, while SF exhibited higher density and heterogeneity. The network that included sodium ion revealed several correlated metabolites, some of which were confirmed by t-test and OPS-DA. Overall, metabolites such as carbohydrates, amino acids, and organic acids corroborated morphophysiological and biochemical results that may help the better performance of SF in comparison to ES. Thus, it provides new insights into the mechanism of salt stress acclimatization related to modulation in primary metabolism in rice cultivars that can be valuable for genotype selection and genetic breeding programs.

Key-words: Salinity. Acclimatization. *Oryza sativa*. Metabolomics.

5 INTRODUCTION

Grains of rice (*Oryza sativa* L.) constitute the diet of more than half of the world's people, and its production reaches approximately 519.5 million tons a year (FAO, 2022). Beyond the Asian continent, Brazil is the largest of rice producer having about 1,619.8 million hectares of cultivated area yielding, almost 11 million tons of grain annually (CONAB, 2022). Overall, the state of Rio Grande do Sul (RS) is responsible for up to 70.7% of the national production of rice (IBGE 2022). However, there are high variations in the electrical conductivity (EC) of rivers ranging from 0.93 to 10.5 dS m^{-1} concerning the total concentration of salts in the water used in rice agriculture (DENARDIN *et al*., 2020). Thus, the soil can be considered saline when the EC reaches 4.0 dS m^{-1}, near 40 mM of NaCl (SHAHID; ZAMAN; HENG, 2018; ZAMLJEN *et al*., 2022).

The presence of salts in the culture media triggers a sequence of physiologically related stresses, such as osmotic stress caused by high concentrations of Na^+ and Cl^-. It decreases the osmotic potential of the soil solution, making it difficult for the roots to uptake water, which result in a decrease in leaf area (NASEER *et al*., 2022). The induction of aggressive saline stress significantly decreases shoot and root length. Likewise, fresh and dry weights of shoots and roots are all decreased, which impacts plant productivity (TANIA *et al*., 2022). In addition to the aforementioned morphological changes, salt stress is also capable of inducing biochemical changes, such as the loss of chlorophyll and carotenoids (YANG *et al*., 2022), photosynthetic inhibition (HASANUZZAMAN; FUJITA, 2022), CO_2 assimilation decrease, light energy excess and the production of reactive oxygen species (ROS) (LIU, C. *et al*., 2022), which act on fatty acids in cell membranes, gradually breaking them down into a series of compounds, including malondialdehyde (MDA) consequence of lipid oxidation (YANG *et al*., 2022).

Plant cells control the levels of ROS through fine-tuning enzymatic and non-enzymatic antioxidant systems such as glutathione, carotenoids, superoxide dismutase (SOD), catalase (CAT), ascorbate peroxidase (APX), and others (MANSOOR *et al*., 2022). For example, SOD is the first line of defense against ROS-mediated damage, catalyzing the disproportion of superoxide anions (O_2^-) to generate hydrogen peroxide (H_2O_2) and O_2. Then, CAT and APX work in the H_2O_2 removal to release H_2O and O_2 (MANSOOR *et al*., 2022; YANG *et al*., 2022). In addition, another way to mitigate the effects of salt stress is through ionic homeostasis since most plants

need to exclude NaCl from the cytoplasm to the apoplast. Otherwise, it provokes cellular toxicity and interferes with the absorption and metabolism of ions essential for salt tolerance, such as K^+, which is critical for plant growth. In rice, salt stress activates the salt overly sensitive (SOS) pathway, activating the *OsSOS1* genes, which mediate root Na^+ uptake and its efflux to the soil (CHEN *et al*., 2021). Besides, the gene family sodium-hydrogen exchanger (NHX) members promote the transport of Na^+ into the vacuole helping to reduce ionic toxicity in the cytosol (KRISHNAMURTHY *et al*., 2019). Indeed, salt tolerance was associated with better growth, photosynthetic maintenance, chloroplast integrity, and ionic homeostasis. It was due to Na^+ exclusion by the upregulation of *OsSOS1, OsSOS2, OsSOS3, OsNHX1, OsNHX2, OsNHX3* and *OsNHX5* gene expressions exhibited by the BRS São Francisco (SF) cultivar in contrast to the BRS Esmeralda (ES) cultivar (GADELHA *et al*., 2021). However, the mechanism of differential tolerance remains to be explored..

Primary metabolism plays an essential in the osmotic adjustment. It is also part of salt tolerance mechanisms the compatible solutes accumulation, such as proline and trehalose. Besides, the overexpressing genes that encode proteins involved in these osmolytes synthesis, such as trehalose-6-phosphate synthase (TPS) and trehalose-6-phosphate phosphatase (TPP) related to the production of trehalose, that helps to relieve the osmotic pressure induced by high salinity (CHEN *et al*., 2021). In addition to the biochemical changes observed in the acclimatization of plants to saline stress, there is a modulation of a wide range of metabolites responsible for various aspects of growth and development under stress (ZANDALINAS *et al*., 2022). The investigation of metabolic changes accompanied by physiological changes provides knowledge about how plants acclimate to stress (SANTOS *et al*., 2022). For example, pepper cultivars growth under saline stress of 20 and 40 mM NaCl showed a modulation of stress-responsive metabolites with a decrease in sucrose, glucose, fructose, organic acids and amino acids metabolism (ZAMLJEN *et al*., 2022).

Since the metabolic data are large and complex, they can be subject to multivariate analysis and interpreted biologically through Cytoscape (PILON *et al*., 2021). It allows us to connect it with morphological, biochemical, and metabolomic parameters represented by nodes that appear connected through edges forming molecular networks. It suggests the models of co-regulated metabolites that help biological statistical inferences (AMARA *et al*., 2022; SHU *et al*., 2022). Thus, the approaches used in this work, such as metabolomics and molecular network analysis

associated with other parameters, may provide new insights into the mechanisms triggered by salt stress acclimation in different rice plant cultivars.

6 MATERIAL AND METHODS

6.1 Plant material and experimental conditions

A previous study showed that the cultivars BRS Esmeralda and São francisco of rice present differential tolerance to saline stress, being sensitive and tolerant, respectively (GADELHA *et al*., 2021). The seeds were provided by Instituto Agronômico de Pernambuco (IPA), Recife - Brazil. The investigation was carried out in the green house of the Plant Physiology laboratory of the Department of Biochemistry and Molecular Biology (DBBM) placed at the Federal University of Ceará (UFC) – Brazil (3°44'41.4"S 38°34'30.7"W).

The seeds were sanitized with sodium hypochlorite (NaClO) 1.0% for 10 minutes. It was washed with abundant distilled water and germinated in 200 mL plastic cups containing vermiculite moistened with distilled water. After seven days, standard-sized seedlings were moved to recipients containing 10 liters of half-strength macro and micronutrient solution with constant aeration (CLARK, 1975). After two days, the plants were placed in a complete strength solution for more seven days, followed by daily pH monitoring, adjusted to 6.5 if necessary and periodic changes (every three days) to avoid nutritional deficiencies (GADELHA *et al.*, 2021). Then, seedlings were transferred to buckets (three plants/buckets) containing three liters of nutrient solution. The treatments were performed in quadruplicate (four buckets containing three plants each) and divided between control (without NaCl addition) and with the addition of 40 mM NaCl for SF and ES. After two days of acclimatization, the nutrient solution was changed and 80 mM of NaCl (final concentration) was added, followed by periodic changes (every three days) to avoid nutritional deficiencies, and daily monitoring of the pH was carried out, adjusted to 6.5 when required. Thus, the data were collected after twelve days of treatment with 80 mM NaCl salinity.

The plant material was collected and divided into leaves, stems, and roots. Part of the material was frozen in liquid nitrogen for future analysis and stored at -80 °C. The other half was fresh measured, dried in an oven at 60°C, and destined for ion analysis.

6.2 Gas exchange and fluorescence parameters

Gas exchange and fluorescence parameters measurements were performed, on the first in fully expanded leaves. Data were determined under a constant concentration of 400 μmol mol^{-1} CO_2 and photosynthetic photon flux density of 1200 μmol photon m^{-2} s^{-1}. The analysis of Gas exchange were: CO_2 assimilation (*A*), stomatal conductance (*gs*), efficiency of ribulose-1,5-bisphosphate carboxylase/oxygenase (Rubisco) (*A*/Ci) and transpiration (Trmmol). The analysis of fluorescence parameters were: Electron transfer rate (ETR), photochemical quenching (PQ = (Fm'− Fs)/(Fm'− Fo')), non-photochemical quenching (NPQ = (Fm – Fm')/Fm'], quantum yield of photosystem II (PSII) (Fv/Fm). The Gas exchange and fluorescence parameters were performed using an infra-red gas analyzer (IRGA, mod. LI-6400XT, LI-COR, Lincoln, USA) (GADELHA *et al.*, 2021).

6.3 Analysis of morphophysiological features

The morphophysiological analysis was performed following Queiroz *et al.* (2020). The length of the shoot and root of the rice were obtained using the ImageJ software and expressed in centimeters per plant (cm $plant^{-1}$). The roots and shoots of each replicate were stored in paper bags and placed in a forced-air circulation oven at 60°C for 72 hours. After drying, shoot dry mass (SDM) and root dry mass (RDM) were measured using an electronic balance. The data were expressed in grams per plant (g $plant^{-1}$).

6.3.1 Determination of íons K^+ e Na^+

For the determination of K^+ and Na^+ ions concentrations, initially, the extracts were obtained by homogenizing 50 mg of powder macerated from dried leaves and roots in 5 mL of distilled water in test tubes. Subsequently, they were kept in a water bath at 95 °C for one hour and shaken every 15 minutes. Then the tubes were centrifuged (3,000 xg for 15 min) at 25°C. The supernatant was collected and stored at -25 °C until use. The contents of Na^+ and K^+ were determined according to Malavolta, Vitti, and Oliveira (1989) in a flame photometer (Micronal®, Model B462). The results are expressed in mmol per gram of dry mass (mmol g^{-1} DM).

6.4 Analysis of biochemical parameters

To assess the effect of salt stress on biochemical parameters, fresh plant material was removed from storage at -80 °C for the following determinations were performed.

6.4.1 Photosynthetic pigments

The determination of chlorophyll (Chl) and carotenoids was performed on the day of data collection, according to Wellburn (1994). Briefly, 16 mg of fresh leaf discs from the first fully expanded rice leaf were placed in a microtube containing 2.0 mL dimethylsulfoxide (DMSO) solution saturated with $CaCO_3$ for 72 hours in the absence of light. Then the samples were incubated in a water bath at 65 °C for 45 minutes. The supernatant absorbances at 665, 649, and 480 nm were measured, whose blank was the extraction solution (Dimethylsulfoxide (DMSO) saturated with CaCO3). The levels of chlorophyll *a* (Chl *a*), *b* (Chl *b*), *total* (Chl *total*), and carotenoids were expressed in mg g^{-1} following the formula:

Chl *a* = 12.47 x A_{665} – 3.62 x A_{649};
Chl *b* = 25.06 x A_{649} – 6.50 x A_{665};
Chl *total* = 7.15 x A_{665} + 18.71 x A_{649};
Carotenoids = (1000 x A_{480} – 1.29 x Chl a – 53.78 x Chl *b*)/220.

6.4.2 Hydrogen peroxide

Rice leaves (200 mg) were immersed and powdered in liquid nitrogen (N_2). It was homogenized in a trichloroacetic acid (TCA) solution (0.1% w/v), centrifuged at 12,000 xg for 15 minutes at 4 °C. Then, 0.8 mL of 10 mM KH_2PO_4 buffer (pH 7.0) and 1.0 M potassium iodide (KI) was added to the supernatant. At the end of the process, H_2O_2 was quantified at 390 nm of absorbance with a standard curve of increasing concentration of H_2O_2 and expressed in μmol H_2O_2 g^{-1} of fresh mass (MF) (VIGHI, 2016).

6.4.3 Malondialdehyde (MDA)

Fresh leaf tissues (200 mg) were pulverized in liquid N_2 and homogenized in 2.0 mL of TCA at (0.1% w/v) at 4 °C. The homogenate was centrifuged at 12,000 xg for 15 minutes at 4°C. The reaction occurred mixing the extract in a 5% (m/v) 2-thiobarbituric

acid (TBA) solution prepared in TCA (20% m/v). The reaction mixture was incubated at 95 °C for 30 minutes, followed by fast cooling in an ice bath for 10 minutes (VIGHI, 2016). The TBA absorbance was measured following the equation:

$[MDA] = (A_{532} – A_{600})/(\varepsilon\ b)$

Being:

ε (molar extinction coefficient = 1.56×10^{-5} cm^{-1});

b (optical length = 1).

Malondialdehyde concentration was expressed in μmol of MDA g^{-1} MF.

6.4.4 Extract for enzymatic activity

The protein extract was obtained by macerating 0.5 g of fresh leaves material in liquid nitrogen and 10 mL of 0.1 M KH_2PO_4 with 0.1 mM EDTA (pH 7.0), at 4 °C using a mortar placed on ice. After 5 minutes of maceration, the homogenate was filtered through fine nylon fabric, transferred to 1.5 mL tubes, and centrifuged at 12,000 xg for 15 minutes at 4°C. The supernatant was stored in an ultra-freezer at -80 °C to perform enzymatic analysis (NAKANO; ASADA, 1981).

6.4.5 Catalase (CAT)

CAT activity (EC 1.11.1.6) was determined through the absorbance declining at 240 nm (due to consumption of H_2O_2) over 300 seconds with successive readings at 50 second intervals (HAVIR; MCHALE, 1987). The reaction consisted of 1,250 μL of 100 mM potassium phosphate buffer pH 7.0 containing EDTA (0.1 mM), added with 100 μL of H_2O_2 (0.5 M) and 150 μL of the diluted extract. The extracts readings were performed in triplicate. The enzymatic activity was calculated using the molar extinction coefficient of H_2O_2 (ε = 36 M^{-1} cm^{-1}) and the results expressed as μmol H_2O_2 mg^{-1} protein min^{-1}.

6.4.6 Ascorbate peroxidase (APX)

APX activity (EC 1.11.1.1) was determined by monitoring the absorbance decay at 290 nm for 300 seconds, with successive readings at 50 second intervals due to ascorbate oxidation (NAKANO; ASADA, 1981). The reaction consisted of 50 μL of ascorbate (15 mM), 50 μL of H_2O_2 (30 mM), 1390 μL of 50 mM potassium phosphate buffer pH 6.0, and 10 μL of the diluted enzymatic extract. The extracts were measured in triplicate and the results expressed in nM H_2O_2 mg^{-1}. For the calculations, the molar

extinction coefficient of ascorbate (ε=2,8 mM^{-1} cm^{-1}) and the reaction stoichiometry (two moles of ascorbate for one mole of H_2O_2) were considered. The results were expressed as μmol H_2O_2 mg^{-1} protein min^{-1}

6.5 Determination of primary Metabolites by GC-MS

Polar metabolite extraction from rice leaves and roots was performed according to Lisec *et al*. (2006), with minor modifications. Briefly, 50 mg of pulverized tissues were weighed and mixed in a solution with methanol, chloroform, and ultrapure water (2:1:2 v/v). Subsequently, 30 µL of ribitol solution 0.2 mg/mL (as internal standard) was prepared in purified ultrapure water in Milli-Q equipment. Then, it was heated at 70 °C for 15 minutes and centrifuged at 12,000 g. An aliquot of 200 µL supernatant was dried in SpeedVac for 12 hours and resolubilized in 20 µL methoxyamine hydrochloride solution in pyridine (10 mg/0.5 mL Pyridin) and kept at 37 °C for 120 minutes for the formation of oximes, to block the interconversion of cyclic structures and acyl from reducing sugars, that is, to avoid mutarotation (GULLBERG *et al*., 2004). Then, 35 µL of N-methyl-N-(trimethylsilyl) trifluoroacetamide (MSTFA) was added to each microtube and placed at 37 °C for 30 minutes.

Chromatograms were obtained using gas chromatography coupled with mass spectrometry (GC-MS, QP-PLUS 2010, Shimadzu, Japan). An aliquot of 1.0 µL sample was automatically injected in split mode (1:10 ratio) in an RTX-5MS capillary column (30 m x 0.25 mm x 0.25 µm) to separate the metabolites. The carrier gas (He) flow rate was 1.2 mL min^{-1}, and the oven was programmed with an initial temperature of 80 °C for 2 minutes, with an increase of 10°C/min to 315 °C. The reaction was maintained at this temperature for 8 minutes. The injection and ion source temperature were maintained at 250 °C, and the mass spectrometer interface temperature was set at 230 °C. The mass spectrometer was operated at 70 eV (electron ionization, EI). The scanning range used was mass-to-charge ratios 40-700 (m/z), initiated after the solvent cut-off time of 4 min. Both chromatogram and mass spectral analysis were analyzed using Xcalibur® 2.1 software.

The identification of compounds was based on their mass spectral retention and fragmentation times following mass spectra in the NIST library, as well as the retention times of standard metabolites previously performed based on Golm's metabolome database. The relative value of each metabolite was determined by dividing their respective higher peak mass area by the higher peak mass area of the internal

standard (ribitol, Sigma-Aldrich) and then dividing it by the fresh mass. The relative quantification of the metabolites for both leaves and roots were separately uploaded to the MetaboAnalyst 4.0 server (http://www.metaboanalyst.ca) for sequence multivariate analysis.

6.6 Determination of metabolic networks by Cytoscape

The metabolic network was built according to Freire *et al*. (2021), where nodes represent the metabolites, and the edges represent the strength of the connection among them by the Debiased sparse partial correlation coefficient (DSPC) (r). The links in red correspond to positive r ($0.85 > r < 1.0$), and in blue, negative r ($-0.85 > r < -1$). The network parameters analyzed were network density, isolated nodes, connected nodes (number of nodes – isolated nodes), and network heterogeneity. To correlate ion content with metabolic modulations induced by salinity in the rice cultivars ES and SF, the content of each stress metabolite was divided by the average of those found in the absence of salt within the cultivar. The networks were designed to restrict the connections to $-0.60 > r < -1.0$, for the links in blue, corresponding to negative r, and red, to positive r ($0.60 > r < 1.0$).

6.7 Experimental design and statistical analysis

The design was completely randomized, following a 2 × 2 factorial scheme, consisting of two cultivars (ES and SF) and two salt treatments control (0 mM NaCl) and salinity (80 mM NaCl). Each treatment consisted of four replications, and the experimental unit consisted of three plants. Data were submitted to analysis of variance (ANOVA), and when significant at $p \leq 0.05$, means were compared using Tukey's test. Statistical analyzes were performed using the Sisvar program (FERREIRA, 2011).

The values of metabolite relative abundance were processed in MetabolAnalyst 5.0 (https://www.metaboanalyst.ca). Data were normalized (log10 and Pareto scaling) before being submitted to one-way ANOVA and Tukey's test ($p < 0.05$). The data were represented by principal component analysis (PCA), scatter plot (S-plot) by orthogonal partial least squares discriminant analysis OPLS-DA, and cluster analysis (grouping hierarchical) by heatmap (Euclidean distance, Ward clustering algorithm). Subsequently, the metabolomic data were normalized again, this time by CorrelationCalculator 1.0.1 (http://metscape.ncibi.org/calculator.html), to create the

metabolic networks through MetScape in the CYTOSCAPE v.3.7.2 software (https: //cytoscape.org/) (SHANNON *et al*., 2003).

7 RESULTS

7.1 Growth parameters

Rice cultivars ES and SF were grown in hydroponic solution in the presence or absence of NaCl to analyze the biochemical, morphological, and metabolic responses and how they are influenced by to salinity tolerance degree. The treatment with 80 mM NaCl for 12 days promoted a significant reduction in plant growth . The shoot length decreased by approximately 44%, regardless of the cultivar (Table 1 and Figure 2). Salinity also reduced the root length in ES by 21.9%. However, there was an increase of 18.8% in the SF roots. Likewise, the salt treatment reduced the dry masses of leaves, roots, and stems. The presence of NaCl in the hydroponic medium also decreased the leaves dry mass by 53.9% and 41.2% in the ES and SF, respectively. The same occurred in the stems of ES and SF, presenting a reduction of 57.1% and 45.5%, respectively. There was a different behavior between the root's dry masses of the two cultivars in which the ES decreased by 50% and SF decreased by only 16%. In total, the decrease in dry mass was 57.7% and 36.4% in cultivars ES and SF, respectively (Table 1 and Figure 2).

Table 1. Growth parameters of both rice cultivars BRS Esmeralda (ES) and BRS São Francisco (SF) in the absence (Control) and presence of NaCl 80 mM (Salt stress). Shoot and root length, as well as leaves, stems, roots, and total dry masses were measured after 12 days of treatment. The values represent a mean of 4 biological replicates. Capital letters compare the control and salt treatments in the same cultivar, and lowercase letters correspond to the same treatment in different cultivars according to the Tukey test ($p < 0.05$).

	BRS Esmeralda				BRS São Francisco			
	Control		Salt stress		Control		Salt stress	
	Mean	t-test	Mean	t-test	Mean	t-test	Mean	t-test
Shoot length (cm plant^{-1})	55.04	Aa	31.15	Ba	59.06	Aa	33.33	Ba
Root lenght (cm plant^{-1})	31.50	Aa	24.60	Bb	22.10	Bb	26.26	Ab
Leaves DM (g plant^{-1})	0.13	Aa	0.06	Ba	0.17	Aa	0.10	Ba
Stems DM (g plant^{-1})	0.07	Ab	0.03	Bb	0.11	Aa	0.06	Ba
Roots DM (g plant^{-1})	0.06	Ba	0.03	Bb	0.06	Aa	0.05	Ba
Total DM (g plant^{-1})	0.26	Ab	0.11	Bb	0.33	Aa	0.21	Ba

Figure 2 - Phenotypic appearance of rice cultivars under control and salt stress (80 mM NaCl) after 12 days of treatment. A) BRS Esmeralda (ES), and B) BRS São Francisco (SF).

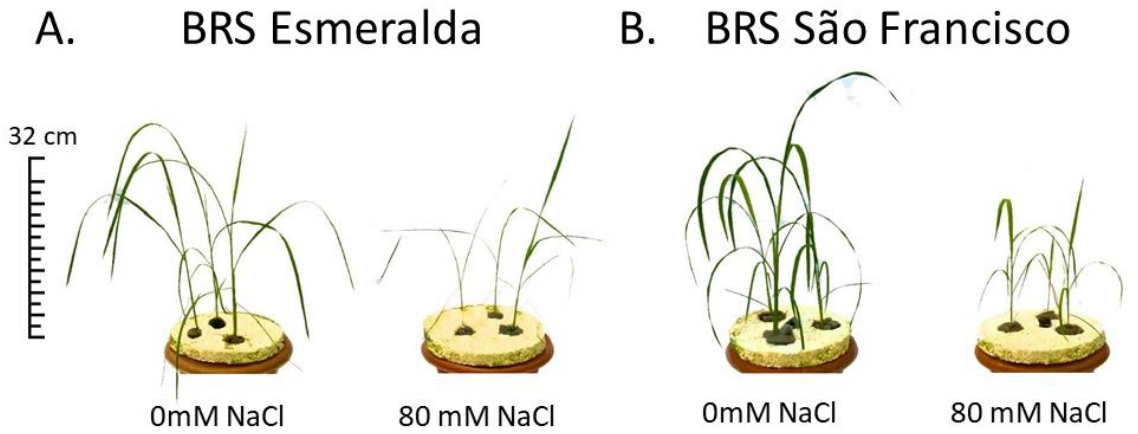

7.2 Pigment contents, gas exchange measurements and fluorescence parameters

Salt treatment affected chlorophyll and carotenoid contents in both ES and SF cultivars (Table 2). Salt reduced the Chl *a* by approximately 31% in the ES cultivar, while in the SF cultivar, there was no statistical difference between the control and saline treatments. The opposite occurred in the Chl *b* content, which showed a decrease of 32% in the SF cultivar, but there was no statistical difference in the ES cultivar. Thus, there was a total chlorophyll depletion of 31.3% and 15.3% in cultivars ES and SF, respectively. Similarly, carotenoid content decreased by 37% and 20% in ES and SF cultivars, respectively (Table 2).

The presence of salt in the nutrient solution substantially decreased the Gas exchange parameters: CO_2 assimilation (*A*), transpiration (*Trmmol*) and stomatal conductance (*gs*), by 70%, 58% and 55%, respectively, for the ES cultivar. The fluorescence parameters: rubisco carboxylation efficiency (*A/Ci*), electron transfer rate (ETR), photochemical quenching (*PQ*), non-photochemical quenching (NPQ) and *Fv/Fm* ratio also decreased to 75%, 50%, 45%, 3% (not significant) and 45%, respectively, for the ES cultivar. On the other hand, the percentages of decrease in these parameters were much smaller in the SF cultivar, which showed reductions of *A*, *Trmmol*, *gs*, *A*/*Ci*, ETR, *PQ*, *NPQ* and *Fv*/*Fm* by 38%, 32%, 48%, 33%, 69%, 21%, 14% and 21%, respectively (Table 2).

Table 2. Photosynthetic and gas exchange traits of both rice cultivars BRS Esmeralda (ES) and São Francisco (SF) in the absence (Control) and presence of NaCl 80 mM (Salt stress). Photosynthetic pigments are represented by chlorophyll *a* (Chl *a*), chlorophyll *b* (Chl *b*), chlorophyll *total* (Chl *t*), and carotenoid contents expressed in $mg.g^{-1}$. Gas exchange traits are represented by Assimilation of CO_2 (*A*) (µmol CO_2 $m^{-2}s^{-1}$), transpiration (*Trmmol*) (mmol H_2O $m^{-2}s^{-1}$), stomatal conductance (*gs*) (mol H_2O $m^{-2}s^{-1}$), rubisco carboxylation efficiency (*A/Ci*) ((µmol CO_2 $m^{-2}s^{-1}$)/(µmol CO_2 mol^{-1})), electron transference rate (*ETR*) (µmol H_2O $m^{-2}s^{-1}$), photochemical quenching of chlorophyll fluorescence [*PQ* = (Fm'-Fs)/(Fm'-Fo')], non-photochemical quenching (NPQ = (Fm – Fm')/Fm'], and quantum yield of photosystem II (PSII) (*Fv/Fm)* were measured after 12 days of treatment. The values represent a mean of 4 biological replicates. Capital letters compare the control and salt treatments in the same cultivar, and lowercase letters correspond to the same treatment in different cultivars according to the Tukey test ($p < 0.05$).

	BRS Esmeralda				BRS São Francisco			
	Control		Salt Stress		Control		Salt Stress	
	Mean	t-test	Mean	t-test	Mean	t-test	Mean	t-test
Chl *a*	2.55	Aa	1.76	Bb	2.66	Aa	2.59	Aa
Chl *b*	1.28	Bb	0.87	Bb	2.29	Aa	1.56	Ba
Chl *total*	3.8	Ab	2.61	Bb	4.83	Aa	4.09	Ba
Carotenoides	0.81	Ab	0.51	Bb	1.06	Aa	0.85	Ba
A	13.55	Ab	4.05	Bb	18.15	Aa	11.23	Ba
Trmmol	7.93	Ab	3.32	Bb	10.31	Aa	6.99	Ba
gs	0.31	Ab	0.14	Bb	0.65	Aa	0.34	Ba
A/Ci	0.04	Ab	0.01	Bb	0.06	Aa	0.04	Ba
ETR	82.78	Ab	41.79	Bb	101.45	Aa	69.57	Ba
qP	0.29	Aa	0.16	Bb	0.33	Aa	0.26	Ba
qN	2.16	Bb	2.10	Ba	2.43	Aa	2.10	Ba
Fv/Fm	0.29	Aa	0.16	Bb	0.33	Aa	0.26	Ba

7.3 Sodium and potassium contents

Salinity increased Na^+ contents in the leaves and roots of both cultivars at 12 days of saline stress (Table 3). Sodium ion contents were increased by 624% and 550% in the leaves, and 214% and 291% in the roots of the ES and SF cultivars, respectively. On the other hand, the contents of potassium ions in leaves decreased by 44% and 24%, and in the root, it decreased by approximately 68% and 30% in ES and SF in this sequence. Thus, the K^+/Na^+ ratio decreased by 93% and 89% in the leaf and presented depletion by 90% and 82% in the root in the cultivar ES and SF, respectively (Table 3).

Table 3. Ion contents of both rice cultivars BRS Esmeralda (ES) and São Francisco (SF) in the absence (Control) and presence of NaCl 80 mM (Salt stress) expressed in (mmol g^{-1} DM). The values of sodium and potassium ions as well as its relations were measured in leaves and roots after 12 days of treatment. The values represent a mean of 4 biological replicates. Capital letters compare the control and salt treatments in the same cultivar, and lowercase letters correspond to the same treatment in different cultivars according to the Tukey test ($p < 0.05$).

	BRS Esmeralda				BRS São Francisco			
	Control		Salt Stress		Control		Salt Stress	
	Mean	t-test	Mean	t-test	Mean	t-test	Mean	t-test
Leaves (Na^+)	6.50	Ba	47.05	Aa	6.20	Ba	40.26	Ab
Roots (Na^+)	11.79	Ba	36.96	Ab	11.08	Ba	43.32	Aa
Leaves (K^+)	28.81	Ab	16.19	Bb	31.93	Aa	24.27	Ba
Roots (K^+)	26.98	Aa	8.74	Bb	23.97	Aa	16.86	Aa
Leaves (K^+/Na^+)	4.66	Aa	0.34	Ba	5.50	Aa	0.61	Ba
Roots (K^+/Na^+)	2.35	Aa	0.23	Ba	2.20	Aa	0.40	Ba

7.4 Malondialdehyde (MDA), hydrogen peroxide (H_2O_2) and enzymatic activity (APX and CAT)

The levels of MDA in leaves under saline stress, an indicator of lipid peroxidation, increased by 211 % in the ES cultivar (Figure 3A). However, there was no significant increase in SF leaves. Comparatively, SF showed lower lipid peroxidation. There were also no significant differences in the peroxide content for both cultivars (Figure 3B). However, APX enzymatic activity increased by 87% in ES, and 55% in SF (Figure 3C), while CAT activity also did not differ significantly between cultivars (Figure 3D).

Figure 3. Biochemical parameters measured in the leaves of ES (Esmeralda) and SF (São Francisco) in the absence (Control) and presence of 80 mM NaCl after 12 days of treatment. Content of malondialdehyde (MDA) (µmol g^{-1} MF) (a), content of hydrogen peroxide (H_2O_2) (µmol g^{-1} MF) (b), activity of ascorbate peroxidase (APX) (µmol min^{-1} mg^{-1} Prot) (c) and activity of catalase (CAT) (µmol min^{-1} mg^{-1} Prot) (d). The values represent a mean of 4 biological replicates. Capital letters compare the control and salt treatments in the same cultivar, and lowercase letters correspond to the same treatment in different cultivars according to the Tukey test ($p < 0.05$).

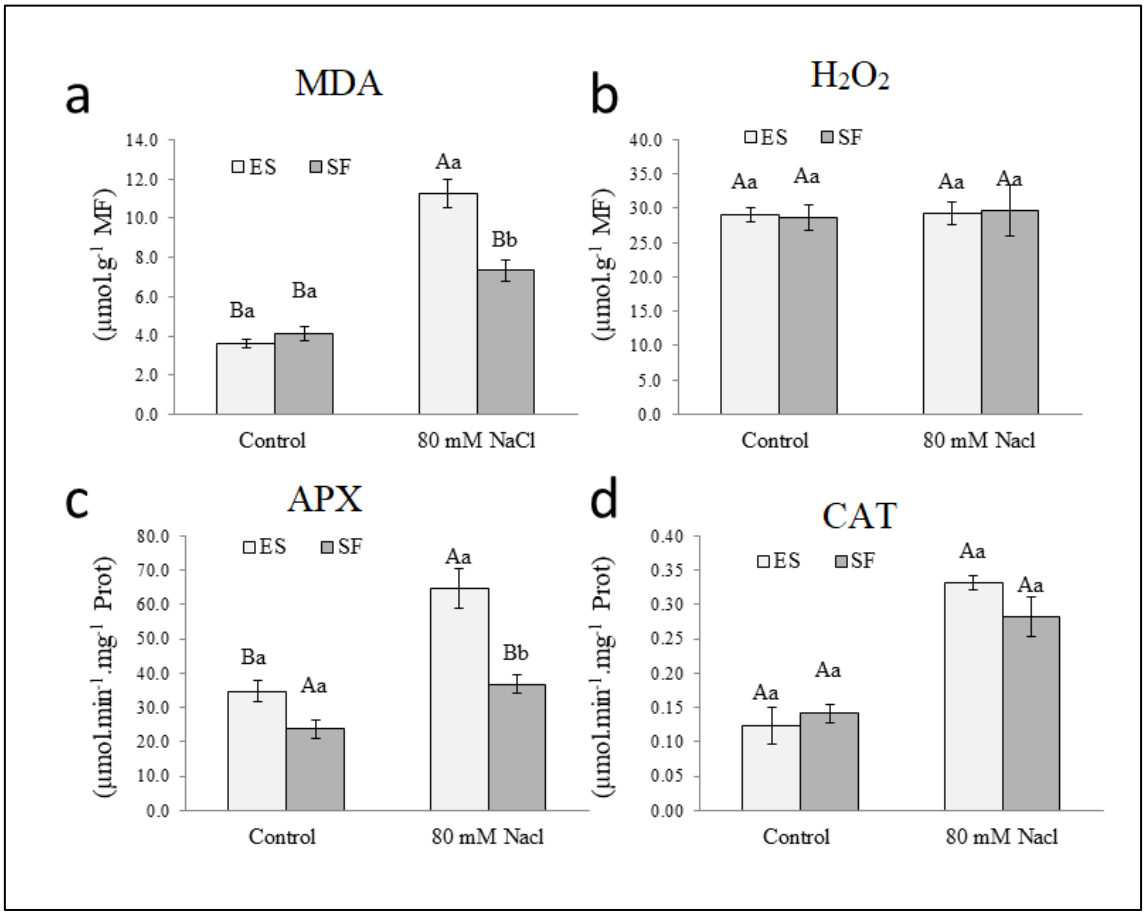

7.5 Metabolic profiles of leaves and roots of rice under salt stress

Changes in the basal metabolism induced by salt stress were investigated in both rice cultivars, ES and SF. Gas chromatography-mass spectrometry (GC-MS) identified the primary metabolites in shoots and roots, and a multivariate analysis was performed. A total of 48 metabolites were identified in leaves and roots based on their mass fragmentation compared to a series of previous standard mass and Golm metabolome database. These metabolites were classified by their compound identification provided in the Kyoto Encyclopedia of Genes and Genomes (KEGG) and the retention times of each one (Table 4). Amino acids were the group with the highest number of metabolites (19), followed by carbohydrates (14), organic acids (9), and other specific groups (6).

Table 4. List of detected metabolites in leaves and roots of rice in the presence and absence of salinity (80 mM NaCl), with their classification in compound types, retention time, and with Kyoto Encyclopedia of Genes and Genomes identifier number (KEGG ID).

Number	Metabolite	Compound type	Retention Time (min)	Compound id
1	Pyruvic acid	Organic acid	7.12	C00022
2	Alanine	Amino acid	8.39	C00041
3	Valine	Amino acid	10.98	C00183
4	Malonic acid	Organic acid	10.73	C00383
5	Serine	Amino acid	11.8	C00065
6	Leucine	Amino acid	12.13	C01933
7	Phosphoric acid	Inorganic acid	12.18	C00009
8	Isoleucine	Amino acid	12.55	C00407
9	Glycine	Amino acid	12.78	C00037
10	Succinic acid	Organic acid	12.87	C00042
11	Glyceric acid	Organic acid	13.28	C00116
12	Fumaric acid	Organic acid	13.45	C00122
13	Threonine	Amino acid	14.29	C00188
14	β-alanine	Amino acid	14.9	C00099
15	Malic acid	Organic Acid	15.98	C00149
16	Methionine	Amino acid	16.45	C00073
17	Proline	Amino acid	16.61	C00148
18	Aspartic acid	Amino Acid	16.48	C00049
19	Pyroglutamic acid	Amino acid	16.49	C01879
20	Threonic acid	Others	17.22	C01620
21	Glutaric acid	Organic acid	17.32	C00217
22	Glutamic acid	Amino acid	17.97	C00025
23	Phenylalanine	Amino acid	18.06	C00079
24	Xylose	Carbohydrate	18.68	C00181
25	Asparagine	Amino acid	18.72	C00152
26	Arabinose	Carbohydrate	18.76	C00216
27	Gulonic acid	Others	19.87	C00800
28	Glutamine	Amino acid	20.12	C00064
29	Shikimic acid	Others	20.60	C00493
30	Ornithine	Amino acid	20.73	C00077
31	Citric acid	Organic acid	20.80	C00158
32	Quinic acid	Others	21.43	C00296
33	Lyxose	Carbohydrate	21.58	C00476
34	Fructose	Carbohydrate	21.74	C02336
35	Mannose	Carbohydrate	21.86	C00159
36	Glucose	Carbohydrate	21.93	C00031
37	Lysine	Amino Acid	22.01	C00047
38	Galactose	Carbohydrate	22.17	C00124
39	Tyrosine	Amino acid	22.25	C00082
40	Glucoheptonic acid	Others	24.24	Not found
41	Inositol	Carbohydrate	24.25	C00137
42	Xylitol	Carbohydrate	24.56	C00379
43	Octadecanoic acid	Organic acid	25.57	C01530
44	Glucopyranoside	Carbohydrate	26.38	C06400
45	Sucrose	Carbohydrate	30.00	C00089
46	Maltotriose	Carbohydrate	31.44	C01835
47	Palatinose	Carbohydrate	31.65	C01742
48	Raffinose	Carbohydrate	31.96	C00492

Principal component analysis (PCA) of metabolites in leaves and roots showed the variation of the components induced by the treatments analyzed in the cultivars ES e SF under conditions control (CNT) and salt stress (SALT) (ES-CNT, ES-SALT, SF-CNT, and SF-SALT) (Figure 4). In leaves, PCA1 and PCA2 responded for 30.2% and 13.8% of the variance, respectively (Figure 4A). It showed four different metabolic profiles since there was no overlapping. Indeed, there was a clear separation of the two treatments based on their confidence interval of the multivariate analysis. Similarly, this separation occurred for the cultivars. However, there is a greater distance between SF-CNT from the other groups, mainly influenced by PC1, while PC2 influenced especially the separation of the SF-SALT group from the others. The loading plots show the contribution of each metabolite for PC discrimination (Figure 4B and supplementary table S1). The top five metabolites that contributed the most to PC1 were octadecanoic acid, pyruvic acid, lyxose, malonic acid, and shikimic acid. While for PC2, they were glucoheptonic acid, asparagine, quinic acid, fumaric acid, and citric acid.

Likewise, a complete separation of the groups occurred in the roots, in which PC1 and PC2 contributed 45.9% and 13.2%, respectively (Figure 4C). Consequently, there was a greater influence of PC1 separating the two cultivars regardless of the treatment and PC2 separating the treatments of each cultivar. The loading plots exhibited the metabolites that influenced the profiles. The top five most positive contributing metabolites were gulonic acid, pyruvic acid, pyroglutamic acid, octadecanoic acid, and proline for PC1, and succinic acid, fumaric acid, maltotriose, malic acid, and shikimic acid for PC2 (Figure 4D, Supplementary table 1).

Figure 4. Bidimensional principal component analysis (PCA) of rice cultivars Esmeralda (ES) and São Francisco (SF) in absence (CNT) and presence of NaCl (80 mM). PCA and loading plot of leaves (A and B) and roots (C and D) are shown. Percentual numbers displayed the variation of each component, and colored ellipsis indicated a confidence interval of 95%. Loading plots indicate positive and negative contribution of each metabolite (rose dots), and the positive top five are named. The detailed information of loading plot was shown in Supplemental Table 1.

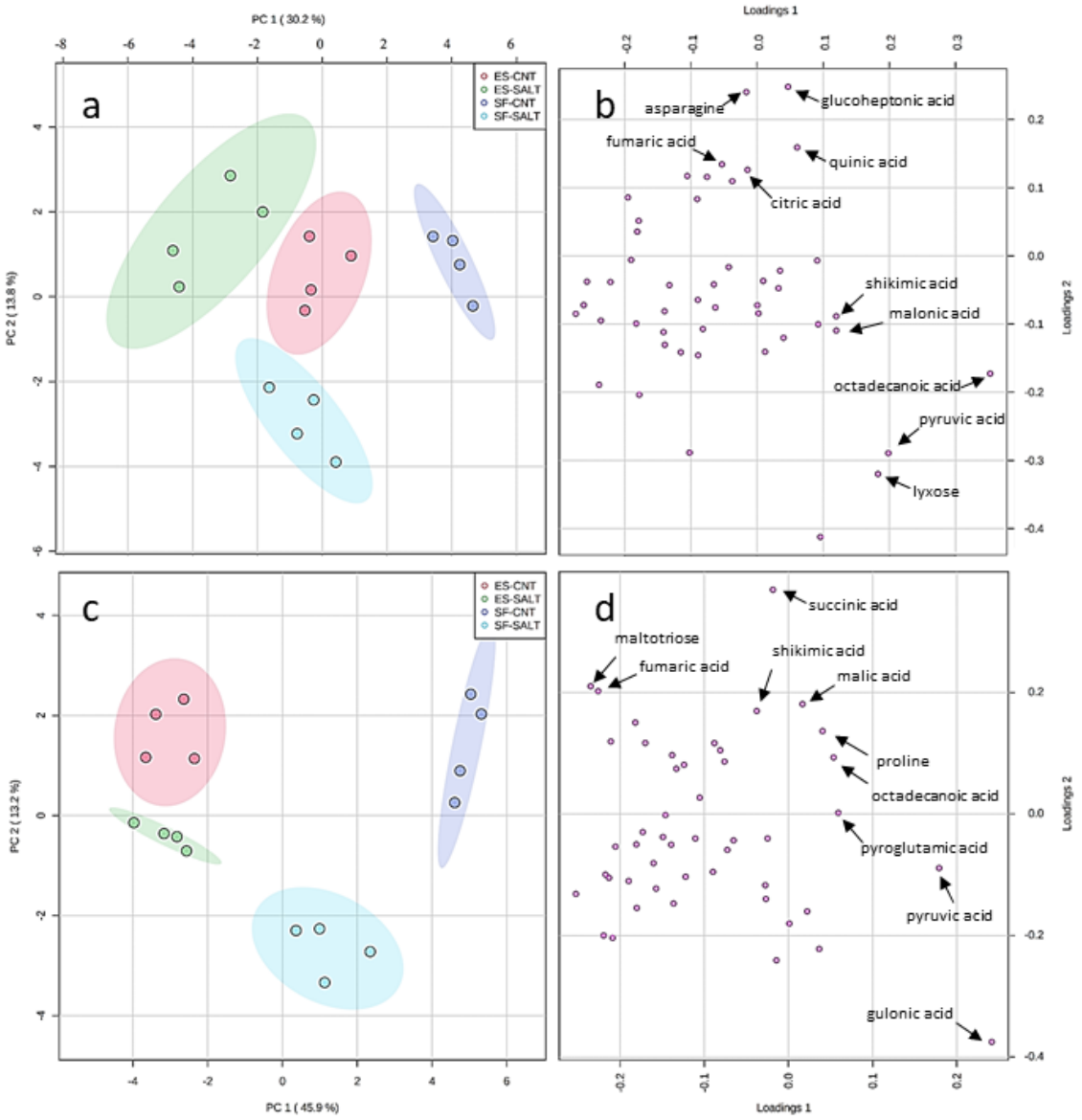

Hierarchical heatmaps by Euclidean distance showed an overview of clustering and positive and negative modulation of different and similar metabolite profiles between treatments based on multivariate analysis (Figure 5). A general trend of positive modulation was observed in both leaves and roots of most metabolites in the SF cultivar compared to their respective control in the absence of salinity. However, a few metabolites in the ES leaves were negatively modulated, mainly of organic acids, such as succinic acid and shikimic acid, and sugars, such as lyxose, mannose, and fructose (Figure 5A, quadrant 1). Conversely, SF exhibited an increase of several metabolites that included organic acids, such as malic acid and aspartic acid, amino acids, for example, β-alanine, isoleucine, and methionine, and sugars, such as maltotriose, raffinose, and galactose (Figure 5A, quadrant 2).

The roots of the ES cultivar showed a tendency to maintain the modulation, without decreasing or increasing, so there were few metabolites exhibiting a positive change. It was included some organic acids, such as glutamic acid and malonic acid, sugars, for example, raffinose and inositol, and amino acids, such as serine (Figure 5B, quadrant 3). On the other hand, several metabolites showed an increase in the SF roots. It includes organic acids, such as glutaric acid, aspartic acid, and phosphoric acid, amino acids, for example, lysine, valine, and β-alanine, and sugars, such as fructose, glucose, sucrose, and mannose (Figure 5B, quadrant 4).

Figure 5. Hierarchical heat maps grouped by Euclidean distance of leaves and roots of the ES and SF in the absence (ES-CNT and SF-CNT) and presence (ES-SALT and SF-SALT) of salt stress. The squares represent the log2 mean of four replicates, and the color map shows an increase (red scale) or decrease (green scale) of each metabolite.

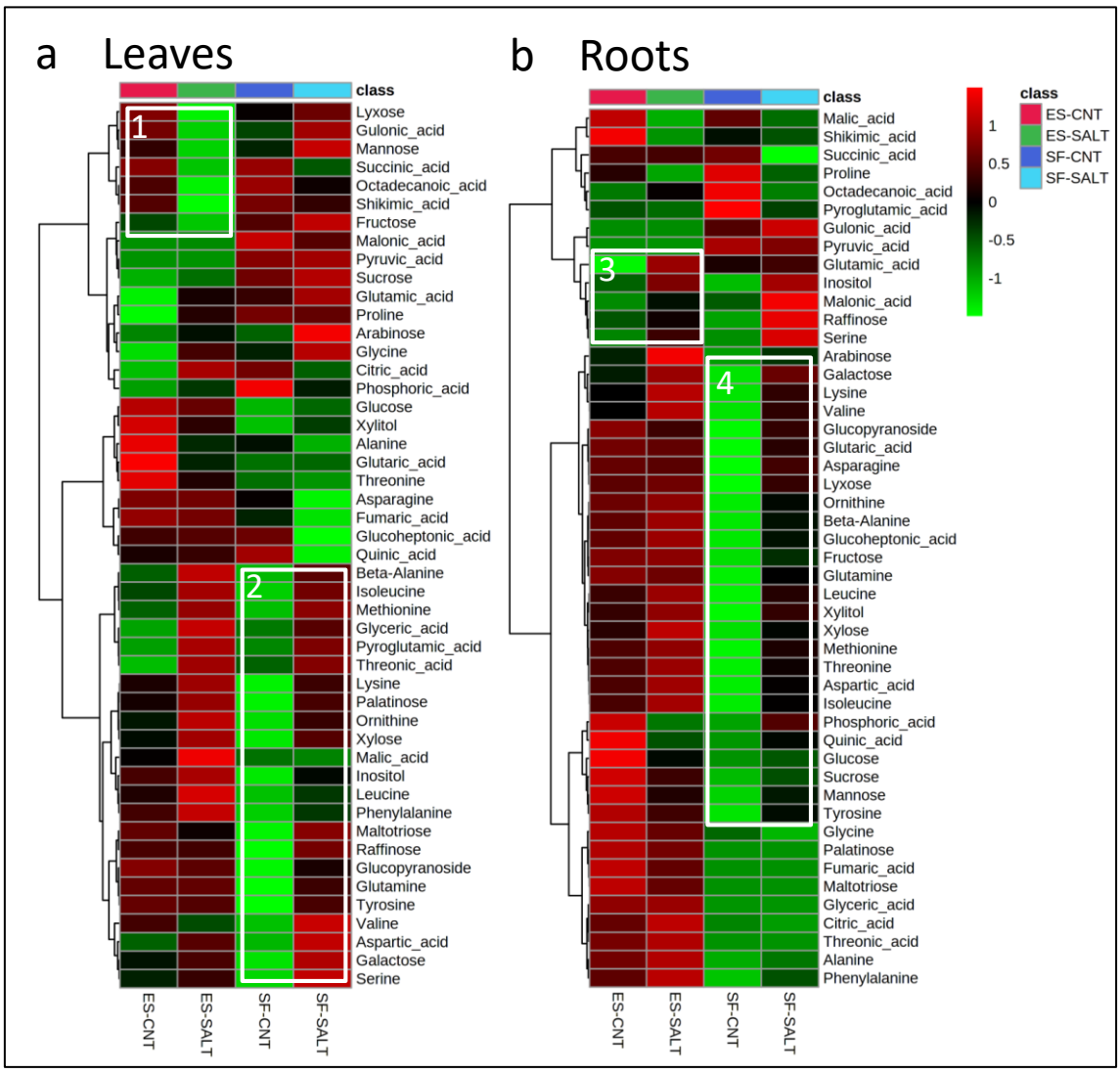

A t-test analysis for each cultivar showed the most significant metabolites with $p<0.05$ (Figure 6), which corroborated the heatmap analysis. In the leaves, 12 metabolites were observed with statistical differences between treatment and control in the ES cultivar (Figure 6A). Six were positively modulated (citric acid, aspartic acid, proline, threonic acid, palatinose, and glyceric acid) and other six were negatively (shikimic acid, mannose, octadecanoic acid, glutaric acid, lyxose, and threonine). Moreover, in the SF cultivar, 19 metabolites exhibited statistical differences. Sixteen were positively modulated (isoleucine, maltotriose, serine, methionine, ornithine, threonic acid, β-alanine, xylose, gulonic acid, glutamine, palatinose, aspartic acid, raffinose, mannose, arabinose, and lysine). Besides, only three were negatively modulated (glucoheptonic acid, fumaric acid, and citric acid) (Figure 6B).

On the other hand, in the roots, nine metabolites were statistically different in the ES cultivar, five positively modulated (β-alanine, glutamic acid, valine, phenylalanine, and leucine) and four negatively modulated (quinic acid, shikimic acid, malic acid, and sucrose) (Figure 6A). While in cultivar SF, 13 were statistically different, only succinic acid was negatively modulated and the other 12 were positively modulated (glutamine, asparagine, leucine, valine, threonine, aspartic acid, glucoheptonic acid, xylitol, glucopyranoside, ornithine, glutaric acid, and methionine when compared to their control treatments (Figure 6D).

Figure 6. Significant difference by t-test ($p<0.05$) between treatments of leaves and roots of rice cultivars ES (A and B) and SF (C and D). The statistics in red represent treatment control (0 mM NaCl), and in green represent salt treatment (80mM NaCl).

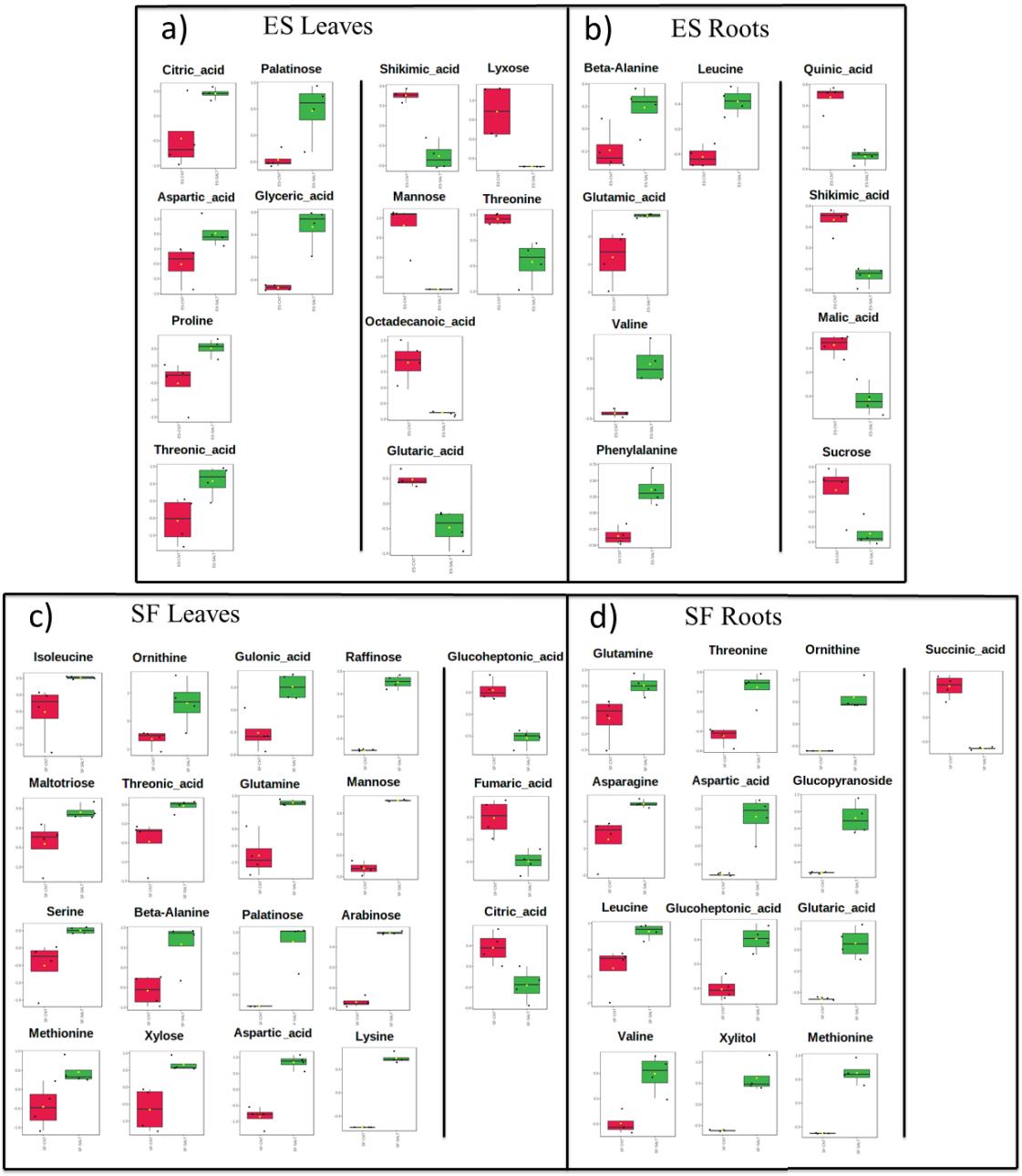

7.6 Identification of potential biomarkers of salt stress in each cultivar under salt stress

The Orthogonal Partial Least Squares Discriminant (OPLS-DA) analysis was performed. The scatter plot (S-plot) showed positive and negative discriminants of each cultivar in the presence of saline stress (80 mM NaCl) compared to the control in the absence of salt (Figure 7). The contribution of probability and correlation were ranked from the highest to the lowest reliability values (Figure 7 and Supplementary table 2). VIP value for ES and SF leaves were greater than 1.2, and 1.1 for leaves and roots, respectively (Supplementary Figure S1). Thus, in leaves of cultivar ES under saline stress compared to the control treatment, the top three main metabolites most discriminating were glyceric acid, palatinose, and threonic acid, and shikimic acid was the most negative (Figure 7A). The same was done for SF leaves, the three most discriminating metabolites were arabinose, lysine, and mannose, and glucoheptonic c acid was the most negative (Figure 7C). In the root of the ES cultivar, the three most discriminating metabolites were leucine, phenylalanine, and valine, with quinic acid being the most negative (Figure 7B). And in the roots of the SF cultivar, the three positive discriminating metabolites were methionine, ornithine, and xylitol, and succinic acid had the most negative impact (Figure 7D).

Figure 7. Scatter plots (S-plot) by orthogonal partial least squares-discriminant analysis (OPLS-DA) of leaves [a (-0.9 > y > 0.9) and c (-1.0 > y > 1.0)] and roots [b (-1.0 > y > 1.0) and d (-1.0 > y > 1.0)] for Esmeralda (a and b) and São Francisco (c and d) cultivars under presence of NaCl in relation to absence of NaCl (treatment/control). The highlighted metabolites which have the top 3 higher values of probability (y) and high correlation in stressed plants are named on the right of S-plot and the most negative on the left for control plants. The detailed information of probability and correlation was shown in Supplemental Table 2.

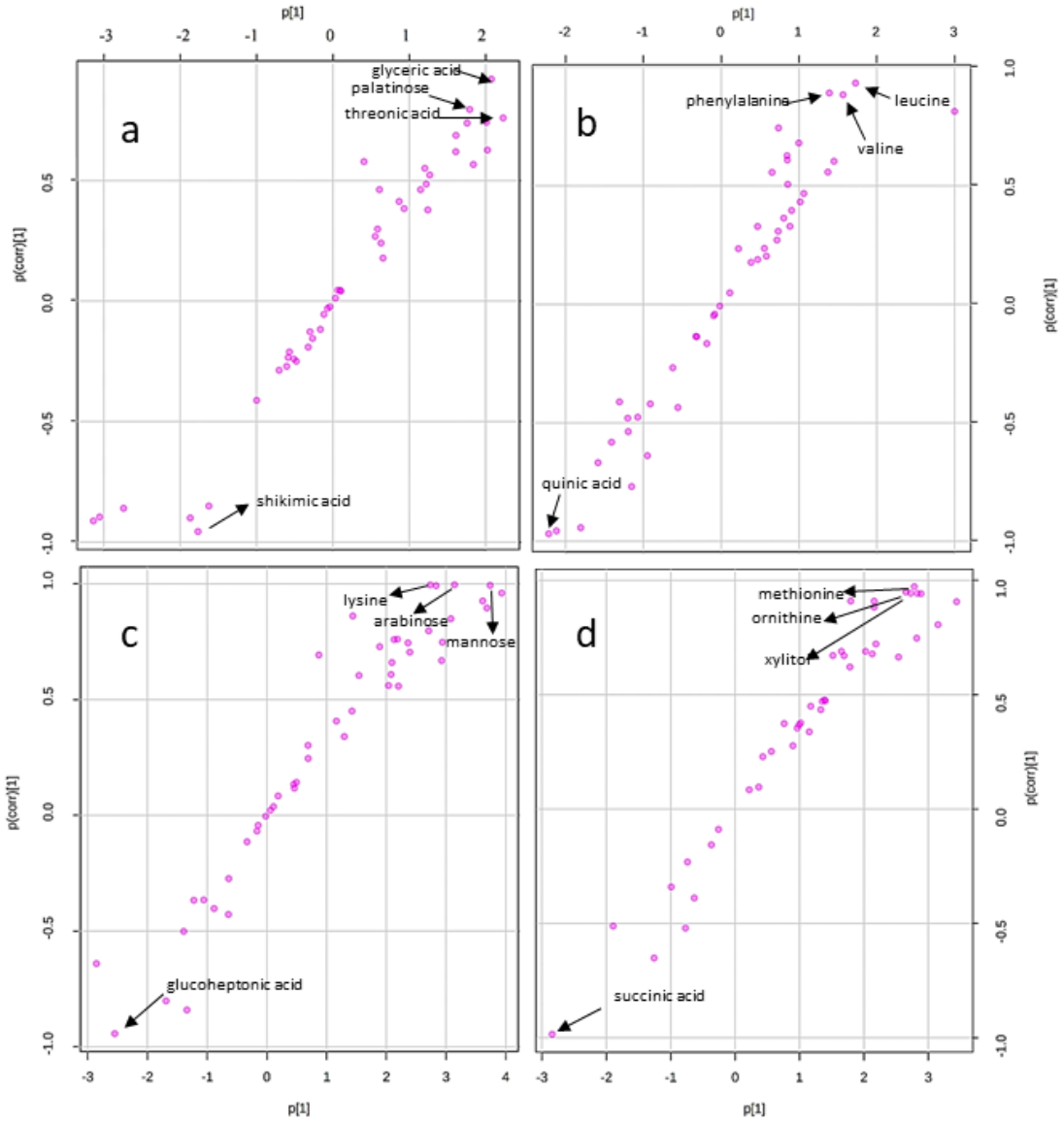

Correlation-based networks demonstrated that the presence of salt in the hydroponic medium of both ES and SF cultivars substantially decreased the topology and the connectivity of their networks of the leaves, with opposite trends observed in the roots (Figure 8). The ES leaf network showed a change from a highly integrated and connected network under control conditions (0 mM NaCl) to a less connected and fragmented network in the presence of salt (Figure 8A). While the SF leaf network showed opposite changes to that observed in ES, its topology changed from a poorly connected and dense network to a highly integrated and connected network under saline stress condition (Figure 8B). The ES root network showed an opposite trend in its topology compared to the application of saline stress on the leaves (Figure 8A), its root metabolites slightly increased the connectivity of its network. The analysis of the metabolic network of the SF roots also showed a similar trend in their topology compared to the application of saline stress on the leaves (Figure 8B), showing a significant increase in their connectivity.

Figure 8. Metabolic networks based on the correlation of metabolomic data from Esmeralda (A) and São Francisco (B) rice cultivars in the presence and absence of salt stress. The networks were created using data on the relative metabolite content of the leaves and roots of rice cultivars. Red links indicate higher *r* (unbiased sparse partial correlation coefficient) in the network, and blue links indicate negative r. Larger nodes indicate a greater degree of connection. These analyzes were performed using CorrelationCalculator software and networks designed using MetScape in CYTOSCAPE software (n = 5).

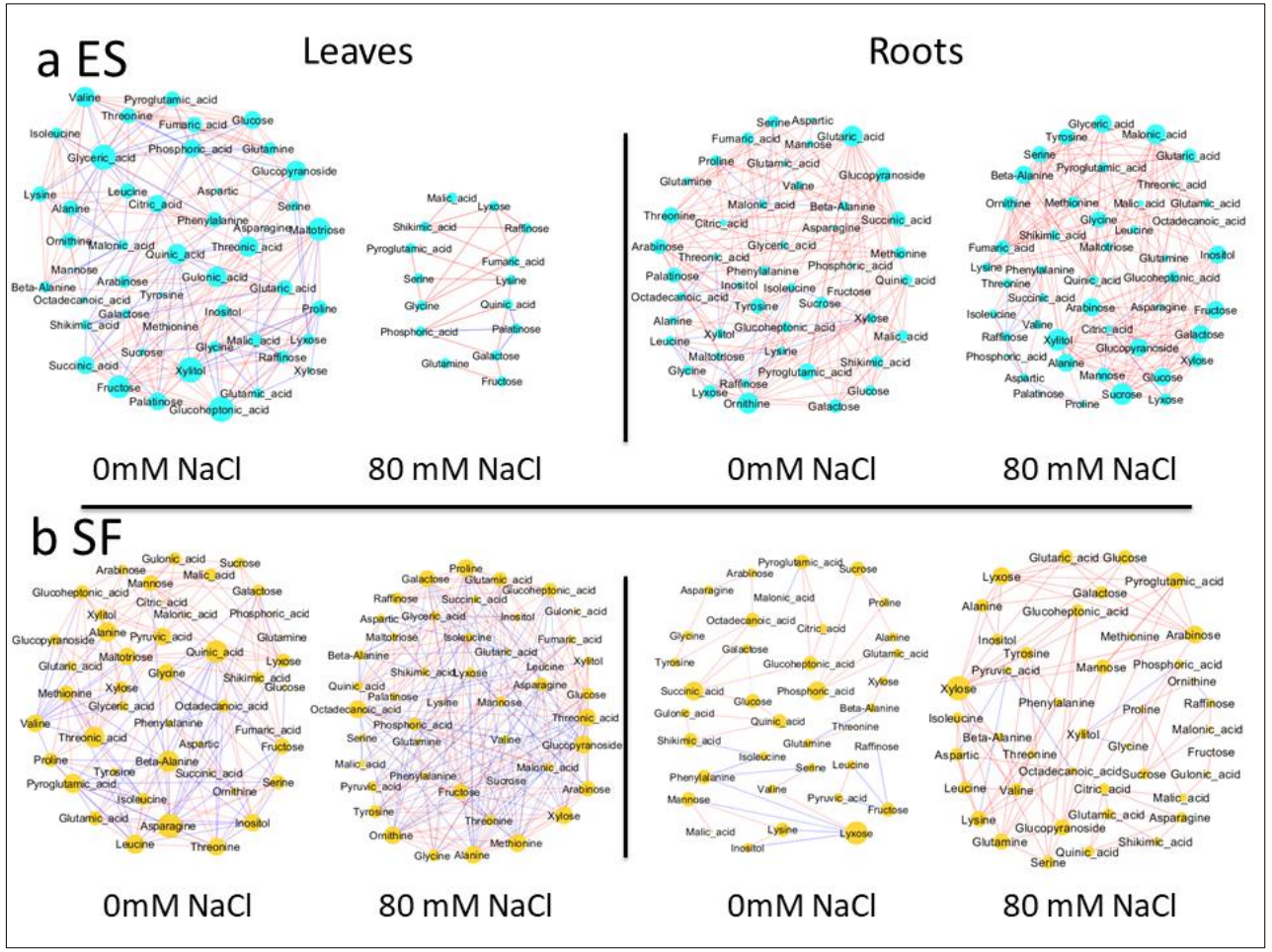

The network of ES leaves showed network density dropping 87% in the presence of salt increasing to 27 the isolated nodes. Additionally, the ES cultivar under salinity had a low connected node (number of nodes – isolated nodes) in 68%. Another clear difference observed between the ES in the absence and presence of stress was related to network heterogeneity. It went up to 346% in ES-SALT, indicating that the nodes had a low degree of connection in the presence of salt (Table 5).

Table 5. Parameters obtained in the analysis of metabolic networks of cultivars of *Oryza sativa L.*, BRS Esmeralda and BRS São Francisco, in the absence (control) and submitted to 80 mM of NaCl (Salt Stress).

	BRS Esmeralda				BRS São Francisco			
	LEAVE		ROOT		LEAVE		ROOT	
	Control	Salt	Control	Salt	Control	Salt	Control	Salt
Network density	0.215	0.027	0.166	0.184	0.176	0.191	0.066	0.108
Isolated nodes	0	27	0	1	1	2	0	0
Connected nodes	47	15	45	45	46	44	37	42
Network heterogeneity	0.337	1.502	0.417	0.423	0.506	0.517	0.357	0.476

The network density of the SF leaves increased up to 9% in the presence of salt. In addition to presenting one and this value increasing to two isolated nodes. It displayed highly connected nodes with 46 connected nodes and greater connectivity than the SF-CNT, which had 44 connected nodes. When comparing the two treatments, the network heterogeneity increased to 2% under stress, indicating that the nodes had a smaller decrease in connection with the presence of salt, different from ES leaves (Table 5).

Under salt stress, the ES roots showed network density increased up to 11%, only 1 isolated node in the presence of salt and highly connected nodes reaching 45. When comparing the two treatments, the network heterogeneity increased to 1% in the presence of salinity, indicating a smaller decrease in the degree of connection under stress (Table 5). while under the same saline stress conditions, the SF roots showed network density increased to 64%, reaching 42 connected nodes, and none was isolated. When comparing the two treatments, the network heterogeneity increased up to 33% in the presence of salinity, indicating a greater decrease in the degree of connection under stress when compared to the ES-SALT root (Table 5).

Metabolites were correlated with Na^+ content in leaves and roots of ES and SF cultivars (Figure 9), to understand how salinity application relates to metabolism products. The networks demonstrate that the presence of salt in the ES culture medium was positively related to most of the metabolites connected in red links. However, at the root of ES, there was greater tendency for Na^+ content to be negatively related to connected metabolites (Figure 9A). Connectivity remains mostly negative when relating SF leaves and roots to salinity (Figure 9B).

The analysis of the metabolic network of the leaves of the cultivar ES shows 34 metabolites positively correlated with the presence of leaf sodium, and only one (palatinose) was negatively correlated (Figure 9A). Nine of these metabolites were significantly related to the t-test (octadecanoic acid, glutaric acid, threonine, citric acid, aspartic acid, proline, threonic acid, palatinose, and glyceric acid). In the SF leaves the number of metabolites decreases to 11, with only four positively related (malic acid, glutaric acid, fumaric acid, and citric acid) and seven negatively (isoleucine, glutamine, β-alanine, aspartic acid, serine, threonine, and phenylalanine) (Figure 9B). Seven of these metabolites were significant in the t-test (fumaric acid, citric acid, isoleucine, serine, β-alanine, glutamine, and aspartic acid).

The analysis of the metabolic network of the ES roots showed 16 metabolites. Three metabolites were positively correlated with the presence of sodium ion (octadecanoic acid, citric acid, and asparagine), and 13 were negatively correlated (galactose, fructose, arabinose, alanine, xylose, xylitol, sucrose, mannose, malonic acid, lyxose, inositol, glucose, and glucoheptonic acid) (Figure 9A). Only one of these metabolites (sucrose) appears as significant in the t-test. In SF roots, the number of nodes raised to 17, but with all metabolites negatively correlated (arabinose, alanine, asparagine, xylose, shikimic acid, serine, quinic acid, pyroglutamic acid, malic acid, lyxose, inositol, gulonic acid, glutaric acid, glucose, galactose, fructose, and citric acid) (Figure 9B). Two of these metabolites (asparagine and glutaric acid) appear as significant in the t-test.

Figure 9. Integration of metabolic data from leaves and roots of rice cultivars Esmeralda (ES) (A) and São Francisco (SF) (B) with Na^+ content. Red links indicate higher *r* (unbiased sparse partial correlation coefficient) in the network, and blue links indicate negative r.

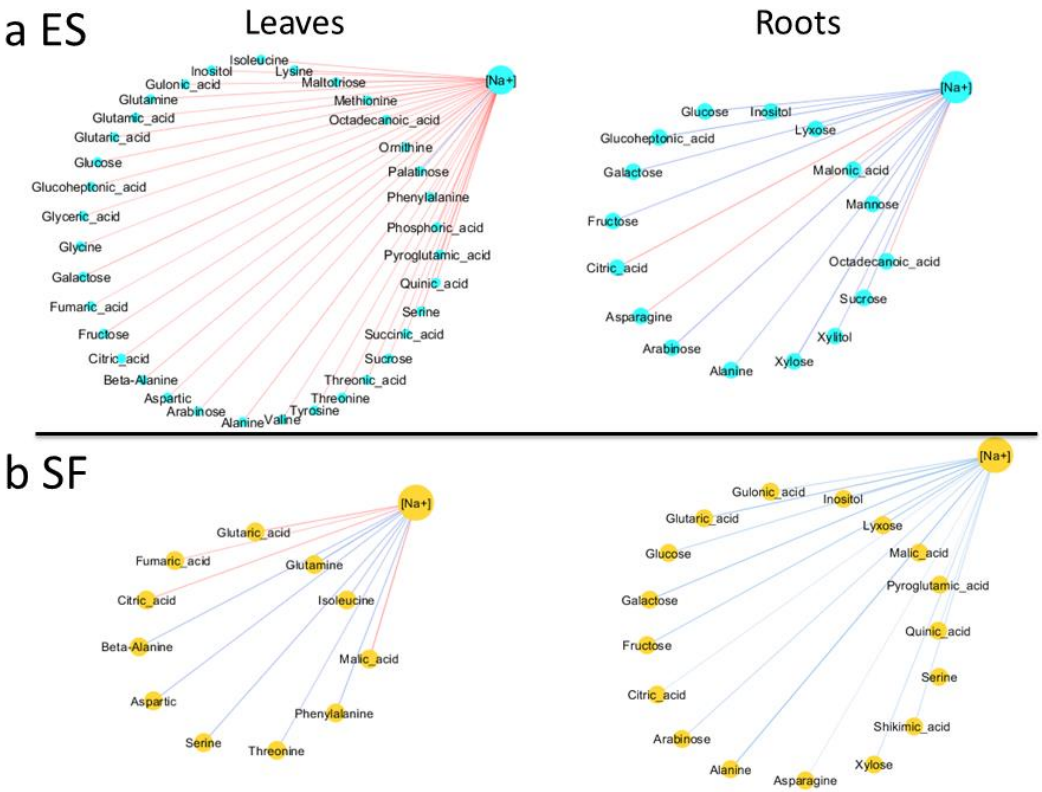

8 DISCUSSION

8.1 BRS Esmeralda and BRS São Francisco cultivars present differential physiological performance to salt stress

Abiotic stresses caused by environmental factors negatively impact crop growth and productivity. The most common abiotic stresses that affect rice farming are drought and salinity (SANTOS *et al.*, 2022). In this case, high salinity in the soil causes visible morphological changes in the plant that mainly include impaired root system, biomass depletion, and plant height decrease, leading to reductions in the yield index (LIU, C. *et al.*, 2022). However, some plants are more salt-tolerant and respond to stress by triggering a protective mechanism and adapting their morphology, physiology, and biochemistry to grow in saline environments (GUO *et al.*, 2022). Thus, the response to salinity is a multigenic complex that involves morphological, physiological, biochemical, metabolic, and molecular alterations. Thus, this work analyzed the morphological, biochemical, and metabolic responses involved in salt acclimation in two rice varieties, BRS Esmeralda (ES) and BRS São Francisco (SF).

Here salinity restricted the growth of rice plants (Figure 2 and Table 1). The literature points out that such reductions are due to the cost of plant acclimatization and ability to respond in the short term to environmental changes through morphological and physiological adjustments, among others, to guarantee its survival, although this process consumes resources of plant growth and development (VILLAGÓMEZ-ARANDA *et al*., 2022). The most severe reductions imposed by salt stress occurred in the ES cultivar, which presented lower root length and dry mass of leaves, stem, and root (Table 1), indicating that this cultivar is more sensitive to salinity than SF, as previously described in other works by Gadelha *et al.* (2021). In addition to having the highest growth rates, SF showed an increase in root length. Studies show that the plant's spontaneous response to increasing its root surface is a way of resisting stress by absorbing more water and nutrients (ARIF; ISLAM; ROBIN, 2019). Salinity promotes reductions in photosynthetic pigments, thylakoid membrane structure damage, increased chlorophyllase activity, and loss of pigmentation protein activity (LIMA *et al.*, 2022). Consequently, degradation of the chloroplast structure promotes a reduction in photosynthetic activity (SHERIN; ASWATHI; PATHUR, 2022). In addition, sodium ions accumulation impairs the absorption of Mg^{+2}, which is essential to synthetize the chlorophyll molecules, also contributing to the inhibition plant growth (RAZIQ *et al.*,

2022). Clearly, there were decrease in photosynthetic parameters under saline stress, but SF exhibited higher levels of chlorophyll *a*, *b*, and *total* compared to ES (Table 2). Thus, SF plants are more photosynthetically active compared to the ES variety. Besides capturing light energy for photosynthesis, carotenoids are antioxidant agents relieving the effect of ROS, minimizing lipid peroxidation in plants exposed to salinity (LIMA *et al*., 2022). Similarly, the higher levels of carotenoids may help a photoprotective action to the photochemical apparatus corroborating the greater performance of SF to salt compared to the ES cultivar. As expected, salt stress also causes stomatal closure, reducing the ability of the leaves to capture atmospheric CO_2 and limiting photosynthetic efficiency (ZAHRA *et al*., 2022). The ES showed more reductions of *A, gs, ETR, A/Ci, PQ, Trmmol*, and the ratio of *Fv*/*Fm* than SF (Table 2). Further, a study involving sweet potato varieties under water deficit stress showed that the tolerant has higher levels of chlorophyll and gas exchange traits, such as *Trmmol* and *gs*, related to high rates of photosynthesis (ZHOU *et al*., 2022).

The high K^+/Na^+ ratio maintenance confers salinity tolerance through ionic homeostasis (HANNACHI *et al.,* 2022). Once inside the cell environment, Na^+ can compete with K^+ for active sites of enzyme transporters, leading to disruption of enzyme function and biosynthesis. Thus, salt-tolerant plants have a higher concentration of K^+ and lower Na^+ in the leaf cytosol (GUO, H. *et al.,* 2022). Here, this study followed the literature since SF plants, which are more tolerant to saline stress, accumulated a lower Na^+ content and a higher K^+ content in the leaves than the ES cultivar under the same conditions (Table 3). The K^+/Na^+ was lower in the leaf and root of SF plants favoring their growth and development in salt treatment since tolerant plants maintain an adequate ratio of cytosolic K^+/Na^+ (GUO, H. *et al.,* 2022). Indeed, SF presents an efficient Na^+ homeostasis system by overexpressing *OsSOS* and *OsNHX* genes related to ion exclusion and vacuole compartmentalization that preserves the chloroplast ultrastructure and photosynthesis (GADELHA *et al.*, 2021).

Salt excess also promoted an increase in MDA levels in ES (Figure 3). However, the SF cultivar did not show an increase in this parameter, and lower MDA levels are reported in tolerant cultivars (SANWAL *et al.*, 2022). Another biochemical indicator of oxidative stress was the H_2O_2 content, but it did not present a significant increase in any of the cultivars. Salinity increased the APX activity in both cultivars but higher in ES (Figure 3), which corroborates with low levels of H_2O_2 registered and its role in the detoxification of this ROS, presenting a greater affinity for H_2O_2 than CAT (SANWAL

et al., 2022). Although these biochemical and molecular mechanisms are known, the part of the modulation of primary metabolites induced by salt stress may reveal possible markers related to the sensitivity and tolerance mechanism in cultivars, and it will be explored next.

8.2 Metabolomic and networks corroborate the adjustments of SF and ES to salt stress

Differences in the modulation of metabolic profiling occur as distinct adaptations in maize plants to improve the salinity tolerance (ARAÚJO *et al.*, 2021). In sorghum, metabolites associated with tricarboxylic acid (TCA) cycle, glycolysis, amino acids, and poliamines were differentially modulate between salt-tolerant and salt-sensible cultivars (OLIVEIRA; LOPES; GOMES-FILHO, 2020). In this study, we also noticed a differential accumulation of metabolites in both leaves and roots of the rice cultivars, BRS São Francisco and BRS Esmeralda, subjected to saline stress. Metabolic profiles under these stress conditions were accessed through the GC-MS analysis technique. The mass pattern of each metabolite allowed the identification of metabolites belonging to the class of free amino acids, organic acids, sugars, and others (Table 4). The multivariate analysis of treatment and cultivars showed different metabolic profiles influenced by different groups of metabolites (Figure 4). The heatmaps exhibited an overview of positive and negative metabolite modulation in both leaves and roots (Figure 5). The t-test also showed this tendency, and a deep analysis showed a higher number of metabolites in the tissues of the SF positively changed under salinity than ES (Figure 6).

The analysis of molecular networks corroborated it, in which the network topology of the ES leaves became less connected and fragmented in the presence of salt (Figure 8A). Otherwise, SF showed a much more robust network, higher density and number of connected nodes under the same conditions (Figure 8B). Indeed, similar results occur in halophytes grown under 400 mM NaCl linking the tolerance to an increase in the network topology of leaves that exhibit high density and connectivity of nodes (PANDA; RANGANI; PARIDA, 2021). The roots showed different results from the leaves. The number of metabolites positively altered under salinity in the ES roots was lower than SF (Figure 5). Similar results reported this differential response after salt stress between tolerant and sensitive rice cultivars, the metabolite modulation was

more evident in roots than shoots, and the tolerant cultivar decrease TCA cycle compounds to increase amino acids (ZUTHER; KOEHL; KOPKA, 2007; BANDEHAGH; TAYLOR, 2020).

Molecular networks showed that under salt, ES cultivar increased the density, in addition to practically maintained its topology (Figure 8A). The cultivar SF shifted from a poorly connected network with few connected nodes to a more robust topology with high connectivity and the appearance of nodes with high heterogeneity (Figure 8B). It corroborated the metabolic profiles and a high amount of positively modulated metabolites compared to the roots of the ES cultivar (Figure 6). Besides, roots of rice cultivars tolerant to osmotic stress present an increase of nitrogen metabolism, carbon, sugars, polyamines, phenylpropanoids and glutathione compared to the sensitive cultivar contributing to the maintenance of biological functions, such as energy generation for antioxidant defense (MATSUNAMI *et al*., 2020). Accordingly, changes in metabolite network topology depend on stress level, and new nodes emerge as hubs in response to plant stress (CARDOSO, FREIRE, DALOSO., 2022). Indeed, roots and shoots of SF increased the density, connectivity, and heterogeneity of metabolite network.

8.3 Increase of amino acids helps rice cultivars to growth under salinity

There were two amino acids positively induced in ES leaves, aspartic acid (Asp) and proline (Pro) (Figure 6A). Pro is produced via ornithine pathway in response to salt stress (CHEN *et al*., 2022). It is osmolyte able to protect cell membranes and ensure the functioning of proteins, in addition to eliminating ROS, inducing plant tolerance (ZHOU *et al*., 2022). Additionally, ES roots also showed positive metabolic modulation of four amino acids, β-alanine (β-Ala), valine (Val), phenylalanine (Phe), and leucine (Leu) (Figure 6A) Three of these amino acids (Val, Phe and Leu) also appear as the most discriminating metabolites in the OPLS-DA analysis (Figure 7B). Although ES under salinity shows the ability to modulate specific metabolites, it was not enough to deal with, like the SF cultivar, since the amino acid increase in the tolerant cultivar was higher. The accumulation of amino acids is widely reported in the literature in plants subjected to abiotic stresses (VIANA *et al*., 2022). An osmotic stress investigation reported much more amino acids in IR 58 than Basilanon the tolerant and sensitive rice cultivars, respectively (MATSUNAMI *et al*., 2020), and salinity inhibits plant growth

primarily by reducing the water potential of the soil solution, inducing osmotic stress, which is a decrease in the ability to absorb water (RANA; MARK, 2008; LIU, H. *et al*., 2022). Clearly, the amino acids modulation is required since promote osmotic balance and osmoprotection, protein biosynthesis, precursors of secondary metabolites, and nitrogen transport among plant tissues (LIANG et al., 2022).

In this hand, in the SF leaves, the amino acids glutamine (Gln), Asp, methionine (Met), ornithine, isoleucine (Ile), serine (Ser), β-Ala and lysine (Lys) showed positive modulation. The increase of some amino acids such as Asparagine (Asn), Aspartato (Asp), Glutamato (Glu) and Gln may be related to the carbon and nitrogen cycle in plants. Thus, the nitrate is reduced to nitrite and later to ammonium which, together with CO_2 used to form sugars (sucrose and glucose) that will be processed to 2-oxoglutarate or α-ketoglutarate through glycolysis and TCA cycle, which can generate Glu and Gln. These amino acids can donate their ammonium to produce Asp and Asn. Then, the increase in the levels of Glu, Gln, Asp and Asn under stress help the protein synthesis maintenance (VIANA *et al.*, 2022). In addition, β-ala production confers protection against osmotic stress and ROS accumulation under abiotic stresses (PARTHSARATHY; SAVKA; HUDSON, 2019). Like β-ala, Ser increases in response to stress conditions, participating in plant growth and development, cell division, and phytohormone regulation (MUTHURAMALINGAM *et al*., 2018; MATSUNAMI *et al*., 2020). Further, the modulation of Lys may also have contributed to the better performance of SF. In bean plants, Lys and Tyrosine (Tyr) improve heavy metal stress conditioning by increasing fresh mass, root length, shoot length, leaf dry mass, soluble proteins, phenolic compounds, flavonoids, as well as reducing MDA content and root electrolyte leakage (MAHMOOD *et al*., 2022). In addition, the amino acid Lys also appears among the most discriminating metabolites in the OPLS-DA analysis (Figure 7C).

Likewise, there were mostly amino acids with positive metabolic modulation in SF roots. Some of the amino acids affected were Asp, Glu, Asparagine (Asn), Leu, Val, Threonine (Thr), Ornithine, and Methionine (Met). Thr is fundamental in the development of tolerance, as it has receptors that detect phytohormones, translating them into stress conditions, in addition to participating in plant growth and development and regulation of plant hormones (VIANA *et al.*, 2022). Similar results show that *Lotus japonicus* seedlings tolerant to salinity had high levels of Thr under stress. Wild barley

(*Hordeum spontaneum*) and cultivated (*H. vulgare*) also showed Thr modulation, in addition to a positive change in Val in the presence of salinity (WU *et al*., 2013; XU; FU, 2022). Polyamines (spermine and spermidine), important to promote tolerance to abiotic stress, are synthesized from Arg or ornithine (GONZÁLEZ-HERNÁNDEZ *et al*., 2022). Two these amino acids (Met and ornithine) appear as the most discriminating metabolites in the OPLS-DA analysis (Figure 7D). Thus, positive amino acids modulation may help SF plants to keep several fundamental processes, for example, in osmoprotection that contributed to the higher root length and ROS homeostasis keeping low levels of MDA (Table 1 and Figure 3).

8.4 TCA intermediates provide energy in sensitive cultivars to survive under salinity

In addition to modulating amino acids, saline stress causes changes in the profile of organic acids and sugars, as a defense mechanism against saline ion toxicity, osmotic stress, water deficits and oxidative stress (RHODES, A-ORCZYK; RICH, 2002; LI, Z. *et al.*, 2022), since acids are intermediates in the production of energy through the respiration process (MA; RYAN; DELHAIZE, 2001; LI, Z. *et al.*, 2022). There is a differential modulation of organic acids between tolerant and sensitive cultivars. For instance, the analysis of the tolerant and sensitive soybean plants showed a tendency of the sensitive to accumulate organic acids involved in the TCA cycle (citric acid, α-ketoglutaric acid and malic acid) in order to provide more energy and survive salt stress, while the tolerant did not need to (YANG *et al*., 2017; LI, Z. *et al.*, 2022). The organic acids positively affected in ES leaves were citric, threonic and glyceric acid (Figure 6A). The increase of these organic acids, for example citric acid may be related to the activity of TCA, carbon demand and ATP supply (WIDODO *et al*., 2009; PANDA; RANGANI; PARIDA, 2021). Two of these organic acids (glyceric acid and threonic acid) are discriminant markers between treatments (control and salt) in the root of the cultivar ES (Figure 7A). The organic acid positively affected in ES roots under saline stress was glutaric acid (Figure 6A). Organic acids are closely related to sugars, as they are one of the by-products of incomplete oxidation of photosynthetic assimilates and may participate in the maintenance of redox balance, generation, and consumption of ATP, among others (IGAMBERDIEV; EPRINTSEV, 2016; ZAMLJEN *et al.*, 2022).

In the SF leaves the positively modulated organic acid was only threonic acid there were few organic acids with a significant increase in the t-test, perhaps because saline stress usually causes a major decrease in organic acids in plant tissues, leaves, stems and roots to keep energy and high levels of sugars (VIANA *et al.*, 2022). SF roots also showed beneficial modulation of glutaric acid, as well as glucoheptonic acid (Figure 6D). Glutaric acid is indicated in the literature as an osmotic regulator and ROS reducer (AROCA, 2012; MORCOL *et al*., 2020), in addition, they are a precursor of TCA cycle metabolites (MAURINO; ENGQVIST, 2015; MORCOL *et al*., 2020). Thus, in this cultivar, organic acids were probably metabolized to other metabolites, with their decrease occurring because of the energy expenditure of saline stress, while in the sensitive species, the observed tendency is for production to predict these expenditures.

8.5 Sugars accumulation in SF is linked to the better photosynthetic efficiency

The modulation of sugars also evidenced the differential behavior between tolerant and sensitive cultivars under salt stress. For example, there is a remarkable increase of sugars in the salt-tolerant sweet sorghum due to its higher photosynthetic performance, protection of chlorophylls, increased sucrose synthetase activity, and inhibition of sucrose consumption compared to the sensitive cultivar (YANG *et al*, 2020; WU *et al*., 2021). Indeed, there was only a positive modulation of palatinose in ES leaves (Figure 6A), which also appears as a discriminating metabolite between ES-SALT/CNT treatments (Figure 7A). Conversely, there were a decrease of sugars, mannose and lyxose (in the leaves) and sucrose (in roots) of ES (Figure 6A and Figure 6B). This may be linked to reduction of CO_2 fixation, transpiration, and chlorophylls affecting photosynthetic rate (Table 2), as well as accumulation, distribution, and translocation of tissue sugar (LOPEZ-BERENGUER, ALCARAZ, CARLOS, 2004; ZAMLJEN *et al.*, 2022). Further, the decrease of sugars and organic acids in ES under saline stress could be because these primary metabolites were consumed for the synthesis of secondary metabolites, such as phenols, defense molecules necessary against ROS (BISTGANI *et al*., 2019; ZAMLJEN *et al*., 2022). Further, in ES roots there is a negative regulation of sucrose result of a decrease in carbon assimilation in the leaves.

On the other hand, SF leaves showed positive modulation of sugars, maltotriose, xylose, palatinose, raffinose, mannose and arabinose which may linked to a better

carbon assimilation (Figure 6C; Table 2). It is widely reported in the literature that the accumulation of soluble carbohydrates can decrease the osmotic potential in plants to facilitate water absorption and ensure normal plant growth under stress conditions. Besides, the accumulation of sugar alcohol as arabinose acts in the oxidative unbalance induced by stressful conditions (KUMARI; PARIDA, 2018; PANDA; RANGANI; PARIDA, 2021). Arabinose and mannose also appear among the most discriminating metabolites in the OPLS-DA analysis (Figure 7C). In SF roots, the sugars xylitol and glucopyranoside were induced by salt stress. Xylitol was the discriminant in the OPLS-DA (Figure 7D). As discussed before, xylitol is reported to play metabolite involved in the salt tolerance in halophytes by regulating oxidative damage (KUMARI; PARIDA, 2018; PANDA; RANGANI; PARIDA, 2021). Thus, the decrease of sugars in the ES cultivar may occur in detriment of consumption for energy production to deal with stress since carbon assimilation was severely impaired. Otherwise, the SF cultivar was able to keep higher levels of carbon assimilation that helped to produce sugars and amino acids to mitigated the effects of salinity.

8.6 Molecular networks are impacted by sodium ion

Metabolic networks of ES leaves showed a positive correlation of many metabolites with Na^+, probably because it impacted multiple metabolic pathways resulting in loses in its growth (Figure 9). It is corroborated by literature reporting that the induction of salt stress sensitivity in wheat seedlings promotes the increase of ROS accumulation, decrease of photosynthesis, whilst the metabolism of amino acids, carbohydrates, CoA biosynthesis, among other metabolic pathways were up-regulated in plants treated with the salt stress (YUE *et al*., 2021). In addition, the citric acid and aspartic acid metabolites, which have significant modulation in the t-test, showed a positive correlation with the application of Na^+ from the leaves in the ES cultivar (Figure 9A). Citric acid may act as an important pathway for ES survive and positively relation to sodium helping them to survive (ARIF *et al*., 2021). Aspartic acid also has the same role, in addition to participating in several metabolic pathways (protein synthesis, nucleotide metabolism, TCA cycle, glycolysis, and hormone biosynthesis) (LEI; ROSSI; HUANG, 2022; HAN *et al*., 2021). As previously discussed, the sensitive cultivars show a general tendency to accumulate TCA cycle intermediates (YANG *et al*., 2017; LI, Z. *et al.*, 2022). Palatinosis also appeared in the correlation network,

however it presented a negative relationship with salinity in this cultivar, precisely because, as already discussed in the previous topic, there was a high consumption of sugars in the ES cultivar. In the roots of the ES cultivar, despite the correlation between some metabolites and the sodium ion, there was no coincidence between the t-test data, as in the previous correlation network results, but it can be observed that sugars such as galactose, fructose, arabinose, xylitol, sucrose, mannose, glucose, among others, show a negative correlation with the application of stress (Figure 9B). Probably because salt stress causes a decrease in sugar content, as observed in the study involving the application of high salinity (100 to 150 mM) in grapefruit, which was able to decrease fructose, glucose, and sucrose (WANG, Y. *et al*., 2022).

In the SF leaves, some of the positively modulated metabolites found in the t-test (Ile, Gln, β-Ala, Asp, Ser) were negatively related to the application of Na^+ in the analysis of metabolic networks (Figure 9B), since the most are amino acids, and their use in regulation, stress signaling and ROS homeostasis under salinity has already been discussed. In addition, β-Ala can be consumed to form pantothenate (Vitamin B5), which is a precursor of Coenzyme A (CoA) (VOET *et al*., 2006; PARTHASARATHY; SAVKAE; HUDSON, 2019). β-Ala can also participate in the synthesis of lignin, phospholipids, and fatty acid biosynthesis and degradation (BROECKLING *et al*., 2005; PARTHASARATHY; SAVKAE; HUDSON, 2019). The analysis of the roots of the SF cultivar showed all metabolites with a negative correlation with the application of Na^+ (Figure 9B). The Asn and glutaric acid metabolites were negatively correlated with Na^+ application but positively modulated in the t-test significance analysis. Glutaric acid probably appears to be consumed in the correlation network because, in addition to promoting osmotic regulation and ROS reduction (AROCA, 2012; MORCOL *et al*., 2020), it is a precursor of the TCA cycle metabolites (MAURINO; ENGQVIST, 2015; MORCOL *et al*., 2020), and as previous discussed, organic acids promoted greater activity of the TCA cycle.

In conclusion, metabolic modulation and network analysis of the roots and leaves corroborated the results of growth, gas exchange, pigments, ions, enzymes, and free radicals, to better understand why the SF cultivar showed higher parameters to salt stress when compared to ES. Metabolic profiles suggest a higher production of sugars in tolerant cultivars. Indeed, SF accumulated xylose, palatinose, rafinose, maltotriose, arabinose, and mannose which may be good options to the development of stress

tolerance in rice. It may allow the development of new strategies of crop breeding to decrease the harmful effects of salt stress in plants under salinity. Overall, this study provides new insights into the mechanism of acclimatization to salt stress and indicates bases of modulation in primary metabolism in rice cultivars that can be used for genotype selection and genetic breeding programs to develop plants more tolerant to environmental stresses.

9 CONSIDERAÇÕES FINAIS

A análise dos perfis metabólicos das raízes e folhas das duas cultivares de arroz, com tolerância diferencial ao estresse salino, mostrou alteração significativamente maior na BRS São Francisco (SF) comparativamente à BRS Esmeralda (ES), e alta densidade e heterogeneidade nas redes moleculares, algo que corroborou com os resultados morfofisiológicos e bioquímicos melhores na cultivar SF, sendo possível compreender mais eficientemente os mecanismos de tolerância da SF contrastante com a ES. Entretanto mais pesquisas ainda se fazem necessárias para compreender as vias de sinalização envolvidas nos processos de aclimatação e tolerância em cultivares de arroz. Um exemplo é o estudo de genomas e sequenciamento para identificação de genes diferencialmente expressos em diferentes cultivares, genes responsivos a estresses abióticos e a análise dos fitormônios como ABA, ácidos jasmônico e salicílico, entre outros, considerados cruciais para o crescimento, desenvolvimento e sobrevivência ao estresse. Em geral, os resultados desse trabalho poderão contribuir para o desenvolvimento de novas estratégias de melhoramento genético para diminuir os efeitos nocivos do estresse salino em plantas. Novas ideias sobre o mecanismo de aclimatação ao estresse indicam que as bases da modulação do metabolismo primário em cultivares de arroz poderão ser usados para seleção de genótipos com tolerância diferencial ao estresse salino bem como serem usados em programas de melhoramento genético.

REFERENCIAS

ALAM, M. D. R.; EHIGUESE, F. O.; VITALE, D.; MARTÍN-DÍAZ, M. L. Oxidative stress response to hydrogen peroxide exposure of *Mytilus galloprovincialis* and *Ruditapes philippinarum*: Reduced embryogenesis success and altered biochemical response of sentinel marine bivalve species. **Environmental Chemistry and Ecotoxicology**, *[s.l.]*, v. 4, p. 97-105, 2022.

AMARA, A.; FRAINAY, C.; JOURDAN, F.; NAAKE, T.; NEUMANN, S.; NOVOA-DEL-TORO, E. M.; SALEK, R. M.; SALZER, L.; SCHARFENBERG, S.; WITTING, M. Networks and Graphs Discovery in Metabolomics Data Analysis and Interpretation. **Front. Mol. Biosci.**, *[s.l.]*, v. 9, 2022.

APRIYANTO, A.; COMPART, J.; ZIMMERMANN, V.; ALSEEKH, S.; FERNIE, A. R.; FETTKE, J. Indication that starch and sucrose are biomarkers for oil yield in oil palm (*Elaeis guineensis Jacq*.). **Food Chemistry**, *[s.l.]*, v. 393, 2022.

APSE, M. P.; BLUMWALD, E. Na^+ transport in plants. **FEBS Lett**, *[s.l.]*, v. 581, p. 2247–2254, 2007.

ARAÚJO, G. S.; PAULA-MARINHO, S. O; PINHEIRO, S. K. P.; MIGUEL, E. C.; LOPES, L. S.; MARQUES, E. C.; CARVALHO, H. H.; GOMES-FILHO, E. H_2O_2 priming promotes salt tolerance in maize by protecting chloroplasts ultrastructure and primary metabolites modulation. **Plant Science**, *[s.l.]*, v. 303, n. 110774, 2021.

ARIF, M. R.; ISLAM, M. T.; ROBIN, A. H. K. Salinity Stress Alters Root Morphology and Root Hair Traits in Brassica napus. **Plants**, *[s.l.]*, v. 8, n. 7, 2019.

ARIF, T. U.; ZAHAN, I.; KARIM, M.; IMRAN, S.; HUNTER, C. T. ; ISLAM, S.; MIA, A.; HANNAN, ABDUL; RHAMAN, M. S.; HOSSAIN, A.; BRESTIC, M.; SKALICKY, M.; MURATA, Y. Citric Acid-Mediated Abiotic Stress Tolerance in Plants. **Int J Mol Sci.**, *[s.l.]*, v. 22, n. 13, p. 7235, 2021.

AROCA, R. **Plant Responses to Drought Stress: From Morphological to Molecular Features**. Berlin: Springer-Verlag, 2012.

BACHANI, J.; MAHANTY, A.; AFTAB, T.; KUMAR, K. Insight into calcium signalling in salt stress response. **South African Journal of Botany**, *[s.l.]*, v. 151, p. 1-8, 2022.

BANDEHAGH, A.; TAYLOR, N. L. Can Alternative Metabolic Pathways and Shunts Overcome Salinity Induced Inhibition of Central Carbon Metabolism in Crops?. **Front. Plant Sci.**, *[s.l.]*, v. 11, n. 1072, 2020.

BASHIR, S. S.; HUSSAIN, A.; HUSSAIN, S. J.; WANI, O. A.; NABI, S. Z.; DAR, N. A.; BALOCH, F. S.; MANSOOR, S. Plant drought stress tolerance: understanding its physiological, biochemical and molecular mechanisms. **Biotechnology & Biotechnological Equipment**, *[s.l.]*, v. 35, n. 1, p. 1912-1925, 2021.

BHATTACHARYA, S.; KUNDU, A. Sugars and sugar polyols in overcoming environmental stresses. *In*: ROYCHOUDHURY, A.; TRIPATHI, D. K. **Protective**

Chemical Agents in the Amelioration of Plant Abiotic Stress. Hoboken, NJ: John Wiley and Sons, p. 71–101, 2020.

BISTGANI, Z. E.; HASHEMI, M.; DACOSTA, M.; CRAKER, L.; MAGGI, F.; MORSHEDLOO, M. R. Effect of salinity stress on the physiological characteristics, phenolic compounds and antioxidant activity of *Thymus vulgaris* L. and *Thymus daenensis* Celak. **Ind. Crops Prod.**, *[s.l.]*, v. 135, p. 311–320, 2019.

BROECKLING, C. D.; HUHMAN, D. V.; FARAG, M. A.; SMITH, J. T.; MAY, G. D.; MENDES, P; DIXON, R. A.; SUMMER, L. W. Metabolic profiling of *Medicago truncatula* cell cultures reveals the effects of biotic and abiotic elicitors on metabolism. **J. Exp. Bot.**, *[s.l.]*, v. 56, p. 323–336, 2005.

CARDOSO, L. L.; FRANCISCO, B. S. F.; DANILO, M. D. Plant Metabolic Networks Under Stress: a Multi-species/Stress Condition Meta-analysis. **Journal of Soil Science and Plant Nutrition**, *[s.l.]*, p. 1-18, 2022.

CHEN, D.; SHAO, Q.; YIN, L.; YOUNIS, A.; ZHENG, B. Polyamine function in plants: metabolism, regulation on development, and roles in abiotic stress responses. **Front. Plant Sci.**, *[s.l.]*, v. 9, n. 1945, 2019.

CHEN, Q.; XIE, H.; WEI, G.; GUO, X.; ZHANG, J.; LU, X.; TANG, Z. Metabolic differences of two constructive species in saline-alkali grassland in China. **BMC Plant Biol.**, *[s.l.]*, v. 22, n. 53, 2022.

CHEN, T.; SHABALA, S.; NIU, Y.; CHEN, Z.; SHABALA, L.; MEINKE, H.; VENKATARAMAN, G.; PAREEK, A.; XU, J.; ZHOU, M. Molecular mechanisms of salinity tolerance in rice. **The Crop Journal**, *[s.l.]*, v. 9, n. 3, p. 506-520, 2021.

CHEN, Y.; LI, E. M.; XU, L. Y. Guide to Metabolomics Analysis: A Bioinformatics Workflow. **Metabolites**, *[s.l.]*, v. 12, n. 357, 2022.

CLARK, R. B. Characterization of phosphatase of intact maize roots. **Journal Agriculture Food Chemistry**, *[s.l.]*, v. 23, p. 458-460, 1975.

CONAB - COMPANHIA NACIONAL DE ABASTECIMENTO. **Acompanhamento da safra brasileira de grãos: SAFRA 2021/2022, 10° levantamento**. Brasília: CONAB, 2022, v. 9, n. 10. p. 1-88.

CONAB - COMPANHIA NACIONAL DE ABASTECIMENTO. **A cultura do arroz**. Brasília: CONAB, 2015, p. 1-180.

DENARDIN, L. G. O.; CARMONA, F. C.; ALVES, L. A.; FLORES, J. P. M.; WEBER, E. J.; MARTINS, A. P.; TIECHER, T.; ANGHINONI, I. Using water with different levels of salinity by paddy fields: a Brazilian case study. **Communications In Soil Science And Plant Analysis**, *[s.l.]*, v. 51, n. 22, p. 2821–2829, 2020.

EMBRAPA – EMPRESA BRASILEIRA DE PESQUISA AGROPECUÁRIA. **BRS Esmeralda: Cultivar de Arroz de Terras Altas com Elevada Produtividade e Maior Tolerância à Seca**. Goías: EMBRAPA, 2014, p. 1-4.

EMBRAPA – EMPRESA BRASILEIRA DE PESQUISA AGROPECUÁRIA. **Nova cultivar de arroz irrigado para o Sub-médio e Baixo São Francisco**. Aracaju: Embrapa, 2000, p. 1-12.

EMBRAPA – EMPRESA BRASILEIRA DE PESQUISA AGROPECUÁRIA. **O arroz de terras altas como estratégia para segurança alimentar, intensificação ecológica e adaptação à mudança do clima: rumo aos objetivos de desenvolvimento sustentável para o milênio**. Goías: Embrapa, 2020, p. 1-15.

FAGERIA, N. K. Nutrient management for improving upland rice productivity and sustainability. **Communications in Soil Science and Plant Analysis**, *[s.l.]*, v. 32, n. 15/16, p. 2603-2629, 2001.

FAL, S.; AASFAR, A.; RABIE, R.; SMOUNI, A.; ARROUSSI, H. E. Salt induced oxidative stress alters physiological, biochemical and metabolomic responses of green microalga *Chlamydomonas reinhardtii*. **Heliyon**, *[s.l.]*, v. 8, p. 1-11, 2022.

FAN, Y.; YIN, X.; XIE, Q.; WANG, Z.; SONG, J.; ZHOU, Y.; JIANG, X. Co-expression of SpSOS1 and SpAHA1 in transgenic Arabidopsis plants improves salinity tolerance**. BMC Plant Biol**., *[s.l.]*, v. 19, n. 74, 2019.

FAO - FOOD AND AGRICULTURE ORGANIZATION OF THE UNITED NATIONS. Food Outlook: Biannual Report on Global Food Markets. Rome: FAO, 2022.

FERREIRA, D. F. Sisvar: a computer statistical analysis system. **Cienc. e Agrotecnol,** *[s.l.]*, v. 35, p. 1039–1042, 2011.

FLOWERS, T. J.; COLMER, T. D. Salinity tolerance in halophytes. **New Phytol**, *[s.l.]*, v. 179, p. 945–963, 2008.

FREIRE, F. B. S.; BASTOS, R. L. G.; BRET, R. S. C.; CÂNDIDO-SOBRINHO, S. A.; MEDEIROS, D. B.; ANTUNES, W. C.; FERNIE, A. R.; DALOSO, D. M. Mild reductions in guard cell sucrose synthase 2 expression leads to slower stomatal opening and decreased whole plant transpiration in *Nicotiana tabacum* L. **Environmental and Experimental Botany**, *[s.l.]*, v. 184, 2021.

GADELHA, C. G.; COUTINHO, Í. A. C.; PINHEIRO, S. K. P.; MIGUEL, E. C.; CARVALHO, H. H.; LOPES, L. S.; GOMES-FILHO, E. Sodium uptake and transport regulation, and photosynthetic efficiency maintenance as the basis of differential salt tolerance in rice cultivars. Environ. **Exp. Bot.**, *[s.l.]*, v. 192, 2021.

GILL, S. S.; TUTEJA, N. Polyamines and abiotic stress tolerance in plants. **Plant Signal. Behav**., *[s.l.]*, v. 5, p. 26–33, 2010.

GONZÁLEZ-HERNÁNDEZ, A. I.; SCALSCHI, L.; VICEDO, B.; MARCOS-BARBERO, E. L.; MORCUENDE, R.; CAMAÑES, G. Putrescine: A Key Metabolite Involved in Plant Development, Tolerance and Resistance Responses to Stress. **Int J Mol Sci**., *[s.l.]*, v. 23, n. 6, p. 2971, 2022.

GULLBERG, J.; MORITZ, T.; SJÖSTRÖM, M.; NORDSTRÖM, A.; JONSSON, P. Design of experiments: an efficient strategy to identify factors influencing extraction

and derivatization of *Arabidopsis thaliana* samples in metabolomic studies with gas chromatography/mass spectrometry. **Analytical Biochemistry**, *[s.l.]*, v. 331, p. 283-295, 2004.

GUO, J.; SHAN, C.; ZHANG, Y.; WANG, X.; TIAN, H.; HAN, G.; ZHANG, Y.; WANG, B. Mechanisms of Salt Tolerance and Molecular Breeding of Salt-Tolerant Ornamental Plants. **Front. Plant Sci.**, *[s.l.]*, v. 13, 2022.

GUO, H.; PU, X.; JIA, H.; ZHOU, Y.; YE, G.; YANG, Y.; NA, T.; WANG, J. Transcriptome analysis reveals multiple effects of nitrogen accumulation and metabolism in the roots, shoots, and leaves of potato (*Solanum tuberosum L.*). **BMC Plant Biol**., *[s.l.]*, v. 22, 2022.

HAN, M.; ZHANG, C.; SUGLO, P.; SUN, S.; WANG, M.; SU, T. L-Aspartate: An essential metabolite for plant growth and stress acclimation. **Molecules**, *[s.l.]*, v. 26, n. 1887, 2021.

HANDA, N.; KOHLI, S. K.; KAUR, R.; SHARMA, A.; KUMAR, V.; THUKRAL, A. K.; ARORA, S.; BHARDWAJ, R. Role of compatible solutes in enhancing antioxidative defense in plants exposed to metal toxicity. *In*: HASANUZZAMAN, M.; NAHAR, K.; FUJITA, M. Plants Under Metal and Metalloid Stress. Singapore: Springer, p. 207–228, 2018.

HANNACHI, S.; STEPPE, K.; ELOUDI, M.; MECHI, L.; BAHRINI, I.; LABEKE, M. C. V. Salt Stress Induced Changes in Photosynthesis and Metabolic Profiles of One Tolerant ('Bonica') and One Sensitive ('Black Beauty') Eggplant Cultivars (*Solanum melongena L.*). **Plants**, *[s.l.]*, v. 11, n. 5, 2022.

HASANUZZAMAN, M.; BHUYAN, M. H. M. B; ANEE, T. I.; PARVIN, K.; NAHAR, K.; MAHMUD, J. A.; FUJITA, M. Regulation of Ascorbate-Glutathione Pathway in Mitigating Oxidative Damage in Plants under Abiotic Stress. **Antioxidants (Basel)**, *[s.l.]*, v. 8, n. 9, p. 384, 2019.

HASANUZZAMAN, M.; FUJITA, M. Plant Responses and Tolerance to Salt Stress: Physiological and Molecular Interventions. **Int. J. Mol. Sci.**, *[s.l.]*, v. 23, 2022.

HAVIR, E. A.; MCHALE, N. A. Biochemical and Developmental Characterization of Multiple Forms of Catalase in Tobacco Leaves. **Plant Physiology**, *[s.l.]*, v. 84, p. 450-455, 1987.

HAZRA, A.; DASGUPTA, N.; SENGUPTA, C.; DAS, S. MIPS: functional dynamics in evolutionary pathways of plant kingdom. **Genomics**, *[s.l.]*, v. 111, p. 1929–1945, 2019.

HU, L.; LU, H.; LIU, Q.; CHEN, X.; JIANG, X. Overexpression of mtlD gene in transgenic Populus tomentosa improves salt tolerance through accumulation of mannitol. **Tree Physiol**., *[s.l.]*, v. 25, p. 1273–1281, 2005.

HUSSAIN, S.; HUSSAIN, S.; ALI, B.; REN, X.; CHEN, X.; LI, Q.; SAQIB, M.; AHMAD, N. Recent progress in understanding salinity tolerance in plants: Story of

Na^+/K^+ balance and beyond. **Plant Physiology and Biochemistry**, *[s.l.]*, v. 160, p. 239-256, 2021.

IGAMBERDIEV, A. U.; EPRINTSEV, A. T. Organic Acids: The Pools of Fixed Carbon Involved in Redox Regulation and Energy Balance in Higher Plants. **Front. Plant Sci.**, *[s.l.]*, v. 7, n. 1042, 2016.

IBGE - INSTITUTO BRASILEIRO DE GEOGRÁFIA E ESTATÍSTICA - IBGE. **Indicadores IBGE: Levantamento Sistemático da Produção Agrícola Estatística da Produção Agrícola**. Rio de janeiro: IBGE, 2022.

KHAN, M. N.; AHMED, I.; DIN, I. U. D.; NOURELDEEN, A.; DARWISH, H.; KHAN, M. Proteomic insight into soybean response to flooding stress reveals changes in energy metabolism and cell wall modifications. **Plos One**, *[s.l.]*, v. 17, n. 5, 2022.

KRISHNAMURTHY, P.; VISHAL, B.; KHOO, K.; RAJAPPA, S.; LOH, C. -S.; KUMAR, P. P. Expression of AoNHX1 increases salt tolerance of rice and Arabidopsis, and bHLH transcription factors regulate AtNHX1 and AtNHX6 in Arabidopsis. **Plant Cell Reports**, v. 38, p. 1299–1315, 2019.

KUMARI, A.; PARIDA, A. K. Metabolomics and network analysis reveal the potential metabolites and biological pathways involved in salinity tolerance of the halophyte *Salvadora persica*. **Environ. Exp. Bot.**, *[s.l.]*, v. 148, p. 85–99, 2018.

LEGRAND, P.; DEMBELE, O.; ALAMIL, H.; LAMOUREUX, C.; MIGNET, N.; HOUZÉ, P.; GAHOUAL, R. Structural identification and absolute quantification of monoclonal antibodies in suspected counterfeits using capillary electrophoresis and liquid chromatography-tandem mass spectrometry. **Anal. Bioanal. Chem**., *[s.l.]*, v. 414, p. 2699-2712, 2022.

LEI, S.; ROSSI, S.; HUANG, B. Metabolic and Physiological Regulation of Aspartic Acid-Mediated Enhancement of Heat Stress Tolerance in Perennial Ryegrass. **Plants**, *[s.l.]*, v. 11, n. 2, p. 199, 2022.

LI, J.; YAN, G.; DUAN, X.; ZHANG, K.; ZHANG, X.; ZHOU, Y.; WU, C.; ZHANG, X.; TAN, S.; HUA, X.; WANG, J. Research Progress and Trends in Metabolomics of Fruit Trees. **Front. Plant Sci.**, *[s.l.]*, v. 13, 2022.

LI, X.; DING, M.; WANG, M.; YANG, S.; MA, X.; HU, J.; SONG, F.; WANG, L.; LIANG, W. Proteome profiling reveals changes in energy metabolism, transport and antioxidation during drought stress in *Nostoc flagelliforme*. **BMC Plant. Biol.**, *[s.l.]*, v. 22, n. 162, 2022.

LI Y, ZENG H, XU F, YAN F, XU W. H^+-ATPases in Plant Growth and Stress Responses. **Annu Rev Plant Biol**., *[s.l.]*, v. 20, n. 73, p. 495-521, 2022.

LI, Z.; CHENG, B.; LIU, W.; FENG, G.; ZHAO, J.; ZHANG, L.; PENG, Y. Global Metabolites Reprogramming Induced by Spermine Contributing to Salt Tolerance in *Creeping Bentgrass*. **Int. J. Mol. Sci.**, *[s.l.]*, v. 23, p. 4472, 2022.

LIANG, X.; WANG, Y.; LI, Y.; AN, W.; HE, X.; CHEN, Y.; SHI, Z.; HE, J.; WAN, R. Widely-Targeted Metabolic Profiling in *Lyciumbarbarum* Fruits under Salt-Alkaline Stress Uncovers Mechanism of Salinity Tolerance. **Molecules**, *[s.l.]*, v. 27, n. 5, 2022.

LIMA, G. S.; PINHEIRO, F. W. A.; GHEYI, H. R.; SOARES, L. A. A.; SOUSA, P. F. N.; FERNANDES, P. D. Saline water irrigation strategies and potassium fertilization on physiology and fruit production of yellow passion fruit. **Rev. Bras. Eng. Agríc. Ambiental**, *[s.l.]*, v. 26, n. 3, p. 180-189, 2022.

LISEC, J.; SCHAUER, N.; KOPKA, J.; WILLMITZER, L.; FERNIE, A. R. Cromatografia em fase gasosa perfil do metabolito baseado em espectrometria de massa em plantas. **Nat. Protoc**., *[s.l.]*, v. 1, p. 387-396, 2006.

LIU, C.; MAO, B.; YUAN, D.; CHU, C.; DUAN, M. Salt tolerance in rice: Physiological responses and molecular mechanisms. **The Crop Journal**, *[s.l.]*, v. 10, n. 1, p. 13-25, 2022.

LIU, H.; LIU, Y.; XU, N.; SUN, Y.; LI, Q.; YUE, L.; ZHOU, Y.; ELE, M. *Chrysanthemum* × *grandiflora* leaf and root transcript profiling in response to salinity stress. **BMC Plant Biol**., *[s.l.]*, v. 22, n. 240, 2022.

LOPEZ-BERENGUER C., ALCARAZ C., CARLOS M. Involvement of sugars in the response of pepper plants to salinity: Effect of calcium application. **Asian J. Plant Sci.**, *[s.l.]*, v. 3, p. 455–462, 2004.

MA, J. F.; RYAN, P. R.; DELHAIZE, E. Aluminium tolerance in plants and the complexing role of organic acids. **Trends Plant Sci**., *[s.l.]*, v. 6, p. 273–278, 2001.

MAHMOOD, S.; WAHID, A.; AZEEM, M.; ZAFAR, S.; BASHIR, R.; BAJWA, M. O. S.; ALI, S. Tyrosine or lysine priming modulated phenolic metabolism and improved cadmium stress tolerance in mung bean (*Vigna radiata L*.). **South African Journal of Botany**, *[s.l.]*, v. 149, p. 397-406, 2022.

MAJUMDER, A. L.; JOHNSON, M. D.; HENRY, S. A. 1L-myo-inositol1-phosphate synthase. **Biochim. Biophys. Acta**, *[s.l.]*, v. 1348, p. 245–256, 1997.

MALAVOLTA, E.; VITTI, G. C.; OLIVEIRA, S. A. **Avaliação do Estado Nutricional das Plantas:** Princípios e Aplicações. Piracicaba: Associação Brasileira para Pesquisa da Potassa e do Fosfato, p. 201, 1989.

MANSOOR, S.; ALI, W. O.; LONE, J. K.; MANHAS, S.; KOUR, N.; ALAM, P.; AHMAD, A.; AHMAD, P. Reactive Oxygen Species in Plants: From Source to Sink. **Antioxidants (Basel)**, *[s.l.]*, v. 11, n. 2, 2022.

MATSUNAMI, M.; TOYOFUKU, K.; KIMURA, N.; OGAWA, A. Osmotic Stress Leads to Significant Changes in Rice Root Metabolic Profiles between Tolerant and Sensitive Genotypes. **Plants**, *[s.l.]*, v. 9, n. 1503, 2020.

MAURINO, V. G.; ENGQVIST, M. K. 2-Hydroxy Acids in Plant Metabolism. **Arabidopsis Book**, *[s.l.]*, v. 13, 2015.

MELO, P. B; CARPINETTI, P. A.; FRAGA, O. T.; RODRIGUES-SILVA, P. L.; FIORESI, V. S.; CAMARGOS, L. F.; FERREIRA, M. F. S. Abiotic Stresses in Plants and Their Markers: A Practice View of Plant Stress Responses and Programmed Cell Death Mechanisms. **Plants**, *[s.l.]*, v. 11, n. 9, 2022.

MITTLER, R.; ZANDALINAS, S. I.; FICHMAN, Y.; BREUSEGEM, F. V. Reactive oxygen species signalling in plant stress responses. **Nat. Rev. Mol. Cell. Biol**, *[s.l.]*, 2022.

MORCOL, T. B.; WYSOCKI, K.; SANKARAN, R. P.; MATTHEWS, P. D.; KENNELLY, E. J. UPLC-QTof-MSE metabolomics reveals changes in leaf primary and secondary metabolism of hop (*Humulus lupulus L.*) plants under drought stress. **Journal of Agricultural and Food Chemistry**, *[s.l.]*, v. 68, n. 49, p. 14698-14708, 2020.

MORZE, J.; WITTENBECHER, C.; SCHWINGSHACKL, L.; DANIELEWICZ, A.; RYNKIEWICZ, A.; HU, F. B.; GUASCH-FERRÉ, M. Metabolomics and Type 2 Diabetes Risk: An Updated Systematic Review and Meta-analysis of Prospective Cohort Studies. **Diabetes Care**, *[s.l.]*, v. 45, n. 4, p. 1013-1024, 2022.

MUNNS, R.; GILLIHAM, M. Salinity Tolerance of Crops: What Is the Cost?. **New Phytologist**, *[s.l.]*, v. 208, p. 668-673, 2015.

MUNNS, R.; JAMES, R. A.; GILLIHAM, M.; FLOWERS, T. J.; COLMER, T. D. Tissue tolerance: An essential but elusive trait for salt-tolerant crops. **Funct. Plant Biol**., *[s.l.]*, v. 43, 1103–1113, 2016.

MUNNS, R.; PASSIOURA, J. B.; COLMER, T. D.; BYRT, C. S. Osmotic adjustment and energy limitations to plant growth in saline soil. **New Phytologist**, *[s.l.]*, v. 225, n. 3, p. 1091-1096, 2020.

MUTHURAMALINGAM, P.; KRISHNAN, S. R.; PANDIAN, S.; MAREESWARAN, N.; ARUNI, W.; PANDIAN, S. K.; RAMESH, M. Global analysis of threonine metabolism genes unravel key players in rice to improve the abiotic stress tolerance. **Sci. Rep.**, *[s.l.]*, v. 8, p. 1–14, 2018.

NAKANO, Y.; ASADA, K. Hydrogen Peroxide Is Scavenged by Ascorbate-Specific Peroxidase in Spinach Chloroplasts. **Plant and Cell Physiology**, *[s.l.]*, v. 22, p. 867-880, 1981.

NASEER, M. N.; RAHMAN, F. U.; HUSSAIN, Z.; AHMAD, I.; ASLAM, M. M.; ASLAM, A.; WAHEED, H.; KHAN, A. U.; IQBAL, S. Effect of Salinity Stress on Germination, Seedling Growth, Mineral Uptake and Chlorophyll Contents of Three *Cucurbitaceae* Species. **Brazilian Archives of Biology and Technology**, *[s.l.]*, v. 65, 2022.

NUCCIO, M. L.; WU, J.; MOWERS, R.; ZHOU, H. P.; MEGHJI, M.; PRIMAVESI, L. F; PAUL, M. J.; CHEN, X.; GAO, Y.; HAQUE, E. M.; BASU, S. S.; LAGRIMINI, L. M. Expression of trehalose-6-phosphate phosphatase in maize ears improves yield in well-watered and drought conditions. **Nat. Biotechnol**., *[s.l.]*, v. 33, p. 862–869, 2015.

OLIVEIRA, D. F.; LOPES, L. D. S.; GOMES-FILHO, E. Metabolic changes associated with differential salt tolerance in sorghum genotypes. **Planta**, *[s.l.]*, v. 252, n. 3, p. 1-18, 2020.

PAGE, T. M.; LAWLEY, J. W. The Next Generation Is Here: A Review of Transcriptomic Approaches in Marine Ecology. **Front. Mar. Sci.**, *[s.l.]*, v. 9, 2022.

PANDA, A.; RANGANI, J.; PARIDA, A. K. Unraveling salt responsive metabolites and metabolic pathways using non-targeted metabolomics approach and elucidation of salt tolerance mechanisms in the xero-halophyte Haloxylon salicornicum. **Plant Physiology and Biochemistry**, *[s.l.]*, v. 158, p. 284–296, 2021.

PARTHSARATHY, A.; SAVKA, M. A.; HUDSON, A. O. The Synthesis and Role of β-Alanine in Plants. **Front. Plant Sci.**, *[s.l.]*, v. 10, p. 921, 2019.

PEDROTTI, A.; CHAGAS, R. M.; RAMOS, V. C.; PRATA, A. P. N.; LUCAS, A. A. T.; SANTOS, P. B. Causas e consequências do processo de salinização dos solos. **Revista Eletrônica em Gestão, Educação e Tecnologia Ambiental**, *[s.l.]*, v. 19, n. 2, p. 1308-1324, 2015.

PILON, A. C.; VIEIRA, N. C.; AMARAL, J. G.; MONTEIRO, A. F.; SILVA, R. R.; SPÍNDOLA, L. S.; CASTRO-GAMBOA, I.; LOPES, N. P. Redes moleculares: uma análise sobre anotações e descoberta de novos ativos. **Quim. Nova**, *[s.l.]*, v. 44, n. 09, 2021.

POONAM, R. B.; HANDA, N.; KAUR, H.; RATTAN, A.; BALI, S.; GAUTAM, V.; SHARMA, A.; OHRI, P.; THUKRAL, A. K.; SIRHINDI, G.; ARORA, S. Sugar signalling in plants: a novel mechanism fordrought stress management. **Water Stress Crop Plants**, *[s.l.]*, v. 11, p. 287–302. 2016.

QUEIROZ, C. S.; PEREIRA, I. M. C.; LIMA, K. R. P.; BRET, R. S. C.; ALVES, M. S.; FILHO, E. G.; CARVALHO, H. H. Combined NaCl and DTT diminish harmful ER-stress effects in the sorghum seedlings CSF 20 variety. **Plant Physiology and Biochemistry**, *[s.l.]*, v. 147, p. 223–234, 2020.

RANA, M.; MARK, T. Mecanismos de tolerância à salinidade. **Annu Rev Plant Biol.**, *[s.l.]*, v. 59, p. 651–81, 2008.

RAZIQ, A.; WANG, Y.; MOHI, U. D. A.; SUN, J.; SHU, S.; GUO, S. A Comprehensive Evaluation of Salt Tolerance in Tomato (*Var*. *Ailsa Craig*): Responses of Physiological and Transcriptional Changes in RBOH's and ABA Biosynthesis and Signalling Genes. **Int. J. Mol. Sci.**, *[s.l.]*, v. 23, p. 1-24, 2022.

RHODES, D.; NADOLSKA-ORCZYK, A.; RICH, P. Salinity, osmolytes and compatible solutes. *In*: LÄUCHLI, A.; LÜTTGE, U. **Salinity: Environment-Plants-Molecules**. Springer: Dordrecht, The Netherlands, p. 181–204, 2002.

ROESSNER U, WAGNER C, KOPKA J, TRETHEWEY RN, WILLMITZER L. Technical advance: simultaneous analysis of metabolites in potato tuber by gas chromatography-mass spectrometry. **Plant J.**, *[s.l.]*, v. 23, n. 1, p. 131-142, 2022.

SANCHEZ, D. H.; LIPPOLD, F.; REDESTIG, H.; HANNAH, M. A.; ERBAN, A.; KRÄMER, U.; KOPKA, J.; UDVARDI, M. K. Integrative Functional Genomics of Salt Acclimatization in the Model Legume *Lotus Japonicus*. **Plant J.**, *[s.l.]*, v. 53, p. 973–987, 2008.

SANTOS, T. B.; RIBAS, A. F.; SOUZA, S. G. H.; BUDZINSKI, I. G. F.; DOMINGUES, D. S. Physiological Responses to Drought, Salinity, and Heat Stress in Plants: A Review. **Stresses**, *[s.l.]*, v. 2, p. 113-135, 2022.

SANWAL, S. K.; KUMAR, P.; KESH, H.; GUPTA, V. K.; KUMAR, A.; KUMAR, A.; MEENA, B. L.; COLLA, G.; CARDARELLI, M.; KUMAR, P. Salinity Stress Tolerance in Potato Cultivars: Evidence from Physiological and Biochemical Traits. **Plants**, *[s.l.]*, v. 11, 2022.

SHAH, W. H.; RASOOL, A.; SALEEM, S.; MUSHTAQ, N. U.; TAHIR, I.; HAKEEM, K. R.; REHMAN, R. U. Understanding the integrated pathways and mechanisms of transporters, protein kinases, and transcription factors in plants under salt stress. **Int. J. Genom**., *[s.l.]*, 2021.

SHAHID, S. A.; ZAMAN, M.; HENG, L. Soil Salinity: Historical Perspectives and a World Overview of the Problem. *In*: ZAMAN, M.; SHAHID, S. A.; HENG, L. **Guideline for Salinity Assessment, Mitigation and Adaptation Using Nuclear and Related Techniques**. Springer, Cham: Switzerland, p. 43–53, 2018.

SHANNON, P.; MARKIEL, A.; OZIER, O.; BALIGA, N. S.; WANG, J. T.; RAMAGE, D.; AMIN, N.; SCHWIKOWSKI, B.; IDEKER, T. Cytoscape: a software environment for integrated models of biomolecular interaction networks. **Genome Res.**, *[s.l.]*, v. 13, p. 2498–2504, 2003.

SHARMA, M.; KUMAR, P.; VERMA, V.; SHARMA, R.; BHARGAVA, B.; IRFAN, M. Understanding plant stress memory response for abiotic stress resilience: Molecular insights and prospects. **Plant Physiology and Biochemistry**, *[s.l.]*, v. 179, p. 10-24, 2022.

SHERIN, G.; ASWATHI, K. P. R.; PUTHUR, J. T. Photosynthetic functions in plants subjected to stresses are positively influenced by priming. **Plant Stress**, *[s.l.]*, v. 4, p 1-12, 2022.

SHU, J.; MA, X.; MA, H.; HUANG, Q.; ZHANG, Y.; GUAN, M.; CHUNYUN, GUAN. Transcriptomic, proteomic, metabolomic, and functional genomic approaches of *Brassica napus* L. during salt stress. **Plos One**, *[s.l.]*, v. 17, n. 3, 2022.

SINGH, P.; CHOUDHARY, K. K.; CHAUDHARY, N.; GUPTA, S.; SAHU, M.; TEJASWINI, B.; SARKAR, S. Salt stress resilience in plants mediated through osmolyte accumulation and its crosstalk mechanism with phytohormones. **Front. Plant Sci.**, *[s.l.]*, v. 13, 2022.

SILVA, A. A. R.; LIMA, G. S.; AZEVEDO, C. A. V.; GHEYI, H. R.; SOARES, L. A. A.; VELOSO, L. L. S. A. Salicylic acid improves physiological indicators of soursop irrigated with saline water. **Rev. Bras. Eng. Agríc. Ambiental**, *[s.l.]*, v. 26, n. 6, p. 412-419, 2022.

SOLIS, C.A.; YONG, M.-T.; ZHOU, M.; VENKATARAMAN, G.; SHABALA, L.; HOLFORD, P.; SHABALA, S.; CHEN, Z.-H. Evolutionary Significance of NHX Family and NHX1 in Salinity Stress Adaptation in the Genus *Oryza*. **Int. J. Mol. Sci.**, *[s.l.]*, v. 23, n. 2092, 2022.

TANIA, S. S.; RHAMAN, M. S.; RAUF, F.; RAHAMAN, M. M.; KABIR, M. H.; HOQUE, M. A.; MURATA, Y. Alleviation of salt-inhibited germination and seedling growth of kidney bean by seed priming and exogenous application of salicylic acid (SA) and hydrogen peroxide (H_2O_2). **Seeds**, *[s.l.]*, v. 1, p. 87–98, 2022.

VIANA, V. E.; ARANHA, B. C.; BUSANELLO, C.; MALTZAHN, L. E.; PANOZZO, L. E.; OLIVEIRA, A. C.; ROMBALDI, C. V.; PEGORARO, C. Metabolic profile of canola (*Brassica napus L.*) seedlings under hydric, osmotic and temperature stresses. **Plant Stress**, *[s.l.]*, v. 3, 2022.

VIGHI, I. L. Estreses abióticos em arroz: respostas moleculares, bioquímicas e fisiológicas. 2016. 112 f. Trabalho de conclusão de curso (Doutorado em fisiologia vegetal) – programa de pós-graduação em fisiologia vegetal, instituto de biologia, universidade federal de pelotas, pelotas, 2016.

VILLAGÓMEZ-ARANDA, A. L.; FEREGRINO-PÉREZ, A. A.; GARCÍA-ORTEGA, L. F.; GONZÁLEZ-CHAVIRA, M. M.; TORRES-PACHECO, I.; GUEVARA-GONZÁLEZ, R. G. Activating stress memory: eustressors as potential tools for plant breeding. **Plant Cell Rep.,** *[s.l.]*, v. 41, p. 1481–1498, 2022.

VOET, D.; VOET, J.; PRATT, C. **Fundamentals of biochemistry: Life at the molecular level**. New York: Wiley, 2006.

WAADT, R; SELLER, C. A.; MUNEMASA, P. H. S.; SCHROEDER, J. I. Plant hormone regulation of abiotic stress responses. **Nat. Rev. Mol. Cell. Biol**., *[s.l.]*, 2022.

WANG, W.; PANG, J.; ZHANG, F.; SUN, L.; YANG, L.; FU, T.; GUO, L.; SIDDIQUE, K. H. M. Salt-responsive transcriptome analysis of canola roots reveals candidate genes involved in the key metabolic pathway in response to salt stress. **Sci. Rep**., *[s.l.]*, v. 12, 2022.

WANG, Y.; FENG, Y.; YAN, M.; YU, J.; ZHOU, X.; BAO, J.; ZHANG, Q.; WU, C. Effect of Saline–Alkali Stress on Sugar Metabolism of Jujube Fruit. **Horticulturae**, *[s.l.]*, v. 8, n. 474, 2022.

WELLBURN, A. R. The spectral determination of chlorophylls *a* and *b*, as well as total carotenoids, using various solvents with spectrophotometers of different resolution. **J. Plant Physiol.**, *[s.l.]*, v. 144, n. 3, p. 307-313, 1994.

WIDODO; PATTERSON, J. H.; NEWBIGIN, E.; TESTER, M.; BACIC, A.; ROESSNER, U. Metabolic responses to salt stress of barley (*Hordeum vulgare L.*) cultivars, Sahara and Clipper, which differ in salinity tolerance. **J. Exp. Bot**., *[s.l.]*, v. 60, p. 4089–4103, 2009.

WU, D.; CAI, S.; CHEN, M.; YE, L.; CHEN, Z.; ZHANG, H.; DAI, F.; WU, F.; ZHANG, G. Tissue Metabolic Responses to Salt Stress in Wild and Cultivated Barley. **PLoS ONE**, *[s.l.]*, v. 8, n. 55431, 2013.

WU, H.; HILL, C. B.; STEFANO, G.; BOSE, J. New Insights Into Salinity Sensing, Signaling and Adaptation in Plants. **Front. Plant Sci.**, *[s.l.]*, v. 11, n. 604139, 2021.

XIAO, Q.; MU, X.; LIU, J.; LI, B.; LIU, H.; ZHANG, B.; XIAO, P. Plant metabolomics: a new strategy and tool for quality evaluation of Chinese medicinal materials. **Chin Med**, *[s.l.]*, v. 17, n. 45, 2022.

XIE, Q.; ZHOU, Y.; JIANG, X. Structure, Function, and Regulation of the Plasma Membrane Na^+/H^+ Antiporter Salt Overly Sensitive 1 in Plants. **Front Plant Sci**., *[s.l.]*, 2022.

XU, Y.; FU, X. Reprogramming of Plant Central Metabolism in Response to Abiotic Stresses: A Metabolomics View. **Int. J. Mol. Sci.**, *[s.l.]*, v. 23, 2022.

YAN, S.; BHAWAL, R.; YIN, Z.; THANNHAUSER, T. W.; ZHANG, S. Recent advances in proteomics and metabolomics in plants. **Mol Horticulture**, *[s.l.]*, v. 2, n. 17, 2022.

YANG, D. S.; ZHANG, J.; LI, M. X.; SHI, L. X. Metabolomics analysis reveals the salt-tolerant mechanism in glycine soja. **J. Plant Growth Regul.**, *[s.l.]*, v. 36, p. 460–471, 2017.

YANG, Z.; LI, J-L.; LIU, L-N.; XIE, Q; SUI, N. Photosynthetic Regulation Under Salt Stress and Salt-Tolerance Mechanism of Sweet Sorghum. **Front. Plant Sci.**, *[s.l.]*, v. 10, n. 1722, 2020.

YANG, Z.; MO, Y.; CHENG, F.; ZHANG, H.; SHANG, R.; WANG, X.; LIANG, J.; LIU, Y.; HAO, B. Antioxidant effects and potential molecular mechanism of action of *Limonium aureum* extract based on systematic network pharmacology. **Front. Vet. Sci.**, *[s.l.]*, v. 8, 2022.

YUE, J.; WANG, Y.; JIAO, J.; WANG, H. Comparative transcriptomic and metabolic profiling provides insight into the mechanism by which the autophagy inhibitor 3-MA enhances salt stress sensitivity in wheat seedlings. **BMC Plant Biol**, *[s.l.]*, v. 21, n. 577, 2021.

ZAHRA, N.; HINAI, M. S. A.; HAFEEZ, M. B.; REHMAN, A.; WAHID, A.; SIDDIQUE, K. H. M.; FAROOQ, M. Regulation of photosynthesis under salt stress and associated tolerance mechanisms. **Plant Physiology and Biochemistry**, *[s.l.]*, v. 178, p. 55-69, 2022.

ZAMLJEN, T.; MEDIC, A.; HUDINA, M.; VEBERIC, R.; SLATNAR, A. Salt Stress Differentially Affects the Primary and Secondary Metabolism of Peppers (*Capsicum annuum L.*) According to the Genotype, Fruit Part, and Salinity Level. **Plants (Basel)**, *[s.l.]*, v. 11, n. 7, 2022.

ZANDALINAS, S. I.; BALFAGÓN, D.; GÓMEZ-CADENAS, A.; MITTLER, R. Plant responses to climate change: metabolic changes under combined abiotic stresses, **Journal of Experimental Botany**, *[s.l.]*, v. 73, n. 11, p 3339–3354, 2022.

ZHANG, H.; ZHANG, Z.; XIONG, Y.; SHI, J.; CHEN, C.; PAN, Y.; XUE, T.; XUE, J.; DUAN, Y. Stearic acid desaturase gene negatively regulates the thermotolerance of

Pinellia ternata by modifying the saturated levels of fatty acids. **Industrial Crops and Products**, *[s.l.]*, v. 166, 2021.

ZHOU, Z.; TANG, J.; CAO, Q.; LI, Z.; MA, D. Differential response of physiology and metabolic response to drought stress in different sweetpotato cultivars. **Plos One**, *[s.l.]*, v. 17, n. 3, 2022.

ZUTHER, E.; KOEHL, K.; KOPKA, J. Comparative Metabolome Analysis of the Salt Response in Breeding Cultivars of Rice. *In*: JENKS, M. A.; HASEGAWA, P. M.; JAIN, S. M. **Advances in Molecular Breeding Toward Drought and Salt Tolerant Crops**. Dordrecht: Springer Netherlands, p. 285–315, 2007.

APPENDIX A - LOADING SCORES OF PRIMARY METABOLITES

Table S1. Loading scores of primary metabolites that contributed to PCA of leaves and roots of rice cultivars in the absence and presence of salt. The metabolites were ranked by the highest contribution for each PC1 and PC2.

Leaves				Roots			
Metabolites	Loadings 1	Metabolites	Loadings 2	Metabolites	Loadings 1	Metabolites	Loadings 2
Octadecanoic_acid	0.352	Glucoheptonic_acid	0.248	Gulonic_acid	0.242	Succinic_acid	0.369
Pyruvic_acid	0.199	Asparagine	0.240	Pyruvic_acid	0.179	Fumaric_acid	0.210
Lyxose	0.183	Quinic_acid	0.159	Pyroglutamic_acid	0.059	Maltotriose	0.202
Malonic_acid	0.120	Fumaric_acid	0.134	Octadecanoic_acid	0.054	Malic_acid	0.181
Shikimic_acid	0.120	Citric_acid	0.126	Proline	0.041	Shikimic_acid	0.170
Mannose	0.096	Malic_acid	0.117	Glutamic_acid	0.037	Palatinose	0.151
Fructose	0.093	Threonine	0.116	Malonic_acid	0.022	Proline	0.137
Phosphoric_acid	0.091	Glutaric_acid	0.110	Malic_acid	0.017	Threonic_acid	0.119
Quinic_acid	0.061	Leucine	0.086	Raffinose	0.001	Glyceric_acid	0.117
Glucoheptonic_acid	0.047	Glucose	0.083	Serine	-0.014	Quinic_acid	0.117
Proline	0.040	Glucopyranoside	0.051	Succinic_acid	-0.018	Glucose	0.105
Alanine	0.035	Phenylalanine	0.036	Phosphoric_acid	-0.025	Citric_acid	0.097
Sucrose	0.033	Lysine	-0.006	Galactose	-0.027	Octadecanoic_acid	0.093
Glycine	0.012	Phosphoric_acid	-0.007	Inositol	-0.027	Glycine	0.086
Succinic_acid	0.009	Inositol	-0.016	Shikimic_acid	-0.038	Sucrose	0.081
Gulonic_acid	0.002	Alanine	-0.022	Arabinose	-0.065	Mannose	0.075
Glutamic_acid	0.0005	Succinic_acid	-0.037	Lyxose	-0.073	Alanine	0.027
Citric_acid	-0.014	Ornithine	-0.038	Glycine	-0.076	Pyroglutamic_acid	0.002
Asparagine	-0.016	β-alanine	-0.038	Glucose	-0.081	Tyrosine	-0.002
Glutaric_acid	-0.037	Xylitol	-0.042	Quinic_acid	-0.088	Phenylalanine	-0.030
Inositol	-0.043	Glyceric_acid	-0.043	Lysine	-0.090	Glucoheptonic_acid	-0.038
Fumaric_acid	-0.053	Sucrose	-0.047	Alanine	-0.105	Phosphoric_acid	-0.040
Valine	-0.063	Pyroglutamic_acid	-0.065	Fructose	-0.111	Fructose	-0.040
Xylitol	-0.065	Glutamine	-0.072	Xylose	-0.122	Arabinose	-0.043
Threonine	-0.076	Glutamic_acid	-0.072	Sucrose	-0.124	Glutamine	-0.050
Maltotriose	-0.082	Valine	-0.076	Mannose	-0.133	β-alanine	-0.050
Serine	-0.089	Isoleucine	-0.081	Valine	-0.137	Ornithine	-0.054
Pyroglutamic_acid	-0.089	Gulonic_acid	-0.084	Citric_acid	-0.138	Lyxose	-0.059
Glucose	-0.090	Palatinose	-0.085	β-alanine	-0.139	Threonine	-0.081
Arabinose	-0.102	Shikimic_acid	-0.089	Tyrosine	-0.146	Pyruvic_acid	-0.089
Malic_acid	-0.105	Xylose	-0.095	Glucoheptonic_acid	-0.149	Lysine	-0.095
Galactose	-0.115	Tyrosine	-0.099	Isoleucine	-0.157	Glutaric_acid	-0.100
Glyceric_acid	-0.133	Fructose	-0.100	Threonine	-0.160	Xylose	-0.103
Methionine	-0.139	Maltotriose	-0.107	Glyceric_acid	-0.170	Glucopyranoside	-0.105
Isoleucine	-0.140	Malonic_acid	-0.110	Phenylalanine	-0.173	Methionine	-0.110
Threonic_acid	-0.141	Threonic_acid	-0.112	Asparagine	-0.180	Inositol	-0.117
Aspartic	-0.178	Proline	-0.120	Glutamine	-0.181	Isoleucine	-0.123
Glucopyranoside	-0.179	Methionine	-0.130	Palatinose	-0.182	Aspartic	-0.131
Phenylalanine	-0.181	Glycine	-0.141	Methionine	-0.190	Galactose	-0.140
Tyrosine	-0.183	Galactose	-0.141	Ornithine	-0.206	Valine	-0.147
Lysine	-0.190	Serine	-0.146	Leucine	-0.209	Asparagine	-0.155
Leucine	-0.195	Octadecanoic_acid	-0.173	Threonic_acid	-0.211	Malonic_acid	-0.160
β-alanine	-0.222	Raffinose	-0.189	Glucopyranoside	-0.213	Raffinose	-0.180
Xylose	-0.236	Aspartic	-0.204	Glutaric_acid	-0.217	Xylitol	-0.200
Raffinose	-0.239	Arabinose	-0.289	Xylitol	-0.220	Leucine	-0.204
Ornithine	-0.257	Pyruvic_acid	-0.289	Maltotriose	-0.226	Glutamic_acid	-0.222
Glutamine	-0.262	Lyxose	-0.320	Fumaric_acid	-0.235	Serine	-0.241
Palatinose	-0.274	Mannose	-0.412	Aspartic	-0.253	Gulonic_acid	-0.375

APPENDIX B - LIST OF METABOLITES IN OPLS-DA

Table S2. List of influence of metabolites in OPLS-DA of rice cultivars subject to salt stress compared to non-salt stress.

ES- Leaves			ES- roots			SF- Leaves			SF- roots		
Metabolites	p[1]	p(corr)[1]	Metabolites	p[1]	p(corr)[1]	Metabolites	p[1]	p(corr)[1]	Metabolites	p[1]	p(corr)[1]
Glyceric_acid	2.074	0.92117	Leucine	1.728	0.93345	Arabinose	3.142	0.99603	Methionine	2.784	0.97268
Palatinose	1.79	0.79519	Phenylalanine	1.390	0.89155	Lysine	2.738	0.99538	Ornithine	2.653	0.9497
Threonic_acid	2.228	0.76022	Valine	1.566	0.88404	Mannose	3.738	0.99345	Xylitol	2.730	0.94419
Proline	1.992	0.75378	Glutamic_acid	3.002	0.81404	Raffinose	2.833	0.99185	Glucopyranoside	2.831	0.94344
Aspartic acid	2.009	0.74182	β-alanine	0.73663	0.74397	Aspartic acid	3.933	0.96009	Glutaric_acid	2.888	0.9422
Citric_acid	1.756	0.7386	Methionine	0.99767	0.68055	Palatinose	3.614	0.92602	Glucoheptonic_acid	1.796	0.91002
Pyroglutamic_acid	1.61	0.68785	Malonic_acid	0.8461	0.62666	Glutamine	3.684	0.89586	Threonine	2.160	0.90939
β-alanine	2.022	0.62669	Threonine	0.85021	0.60896	Gulonic_acid	1.440	0.86103	Aspartic acid	3.441	0.90722
Xylose	1.608	0.61985	Xylitol	1.450	0.60349	Xylose	3.080	0.84917	Valine	2.161	0.88286
Sucrose	0.4057	0.57891	Aspartic acid	1.372	0.55774	β-alanine	2.709	0.79666	Leucine	3.152	0.80674
Ornithine	1.838	0.56698	Glucoheptonic_acid	0.65373	0.55658	Threonic_acid	2.186	0.76064	Asparagine	2.822	0.74763
Lysine	1.203	0.55108	Citric_acid	0.85596	0.50605	Methionine	2.130	0.75924	Glutamine	2.187	0.72212
Methionine	1.266	0.52346	Serine	1.062	0.46738	Ornithine	2.939	0.74781	Serine	2.027	0.68986
Leucine	1.220	0.48565	Xylose	1.016	0.43209	Serine	2.363	0.74477	Lysine	1.652	0.68985
Phosphoric_acid	0.60831	0.46267	Arabinose	0.9048	0.39584	Maltotriose	1.889	0.72843	Isoleucine	2.130	0.67874
Phenylalanine	1.147	0.46246	Threonic_acid	0.80479	0.36353	Isoleucine	2.393	0.70475	β-alanine	1.519	0.67175
Glutamic_acid	0.86614	0.4134	Inositol	0.88338	0.32891	Glutamic_acid	0.86996	0.69256	Tyrosine	1.693	0.67087
Malic_acid	0.93139	0.38408	Alanine	0.46799	0.32827	Tyrosine	2.927	0.66851	Gulonic_acid	2.539	0.66496
Isoleucine	1.241	0.37842	Isoleucine	0.73233	0.30797	Valine	2.093	0.66005	Raffinose	1.784	0.62153
Serine	0.58367	0.29888	Lysine	0.71762	0.27113	Galactose	2.079	0.60845	Inositol	1.389	0.47796
Galactose	0.55326	0.26883	Galactose	0.55587	0.23584	Glyceric_acid	1.542	0.60412	Xylose	1.401	0.4733
Glycine	0.62884	0.24122	Glyceric_acid	0.2218	0.23463	Lyxose	2.038	0.56054	Mannose	1.353	0.4718
Arabinose	0.65488	0.17855	Octadecanoic_acid	0.58142	0.20315	Glucopyranoside	2.203	0.55791	Lyxose	1.175	0.45006
Malonic_acid	0.060127	0.045431	Raffinose	0.46897	0.18852	Pyroglutamic_acid	1.425	0.45037	Malonic_acid	1.332	0.43499
Quinic_acid	0.093666	0.044782	Ornithine	0.38511	0.17683	Leucine	1.164	0.40698	Galactose	1.018	0.37681
Glucoheptonic_acid	0.10215	0.041669	Fructose	0.11174	0.0483	Phenylalanine	1.296	0.34028	Sucrose	0.7625	0.37414
Inositol	0.032688	0.012837	Lyxose	-0.01779	-0.00753	Xylitol	0.68962	0.302	Quinic_acid	0.99292	0.36853
Glutamine	-0.04024	-0.02334	Succinic_acid	-0.08142	-0.04118	Fructose	0.69129	0.24556	Fructose	0.96603	0.35449
Asparagine	-0.07177	-0.03036	Asparagine	-0.09644	-0.04868	Pyruvic_acid	0.49535	0.14227	Phenylalanine	1.152	0.33804
Raffinose	-0.11876	-0.05487	Glutaric_acid	-0.32473	-0.13524	Glucose	0.44965	0.13381	Phosphoric_acid	0.89826	0.27722
Fumaric_acid	-0.16459	-0.11727	Glutamine	-0.31425	-0.13707	Glycine	0.46023	0.11729	Glutamic_acid	0.56337	0.25216
Maltotriose	-0.30088	-0.12714	Pyroglutamic_acid	-0.18484	-0.16576	Inositol	0.18836	0.083521	Arabinose	0.43081	0.22934
Tyrosine	-0.26768	-0.15473	Proline	-0.62198	-0.2677	Sucrose	0.1107	0.037467	Glucose	0.36742	0.09643
Alanine	-0.32412	-0.19074	Glucose	-1.308	-0.41177	Glutaric_acid	0.058559	0.021689	Alanine	0.22013	0.084737
Fructose	-0.57022	-0.21097	Tyrosine	-0.91121	-0.42045	Malic_acid	-0.01898	-0.00404	Citric_acid	-0.25798	-0.0884

Succinic_acid	-0.58589	-0.23389
Glucose	-0.51277	-0.23954
Glucopyranoside	-0.4802	-0.24952
Xylitol	-0.60611	-0.27057
Valine	-0.7046	-0.28673
Gulonic_acid	-0.99896	-0.41154
Threonine	-1.625	-0.85001
Lyxose	-2.741	-0.85947
Octadecanoic_acid	-3.055	-0.89571
Glutaric_acid	-1.868	-0.89974
Mannose	-3.136	-0.91184
Shikimic_acid	-1.767	-0.95608

Glycine	-0.55579	-0.43568
Glucopyranoside	-1.072	-0.47652
Mannose	-1.200	-0.48073
Phosphoric_acid	-1.194	-0.53724
Maltotriose	-1.409	-0.58181
Palatinose	-0.94859	-0.63886
Fumaric_acid	-1.583	-0.66833
Sucrose	-1.151	-0.76918
Malic_acid	-1.805	-0.94272
Shikimic_acid	-2.117	-0.95631
Quinic_acid	-2.216	-0.96829

Alanine	-0.14509	-0.04341
Proline	-0.1651	-0.06779
Threonine	-0.33112	-0.11438
Succinic_acid	-0.6382	-0.27338
Phosphoric_acid	-1.057	-0.36567
Asparagine	-1.223	-0.36712
Malonic_acid	-0.88346	-0.40265
Shikimic_acid	-0.64298	-0.42838
Quinic_acid	-1.392	-0.50144
Octadecanoic_acid	-2.853	-0.64062
Citric_acid	-1.688	-0.80172
Fumaric_acid	-1.338	-0.84099
Glucoheptonic_acid	-2.546	-0.94317

Glycine	-0.36849	-0.15605
Pyroglutamic_acid	-0.73893	-0.23102
Proline	-0.99238	-0.34022
Shikimic_acid	-0.63424	-0.38838
Octadecanoic_acid	-1.894	-0.51107
Pyruvic_acid	-0.77104	-0.52013
Malic_acid	-1.258	-0.65094
Succinic_acid	-2.842	-0.98436

APPENDIX C - VIP SCORES

Figure S1. VIP scores related to leaf (a and c) and root (b and d) metabolites of rice cultivars ES and SF in the presence and absence of salt. The heat map with the red and blue squares indicates the high or low concentration, respectively, of the metabolites. The VIP score was based on the orthoPLS-DA model and metabolites with VIP > 1.0 were considered determinants.